# An energy stable fourth order finite difference scheme for the Cahn-Hilliard equation

Kelong Cheng * Wenqiang Feng† Cheng Wang‡ Steven M. Wise§

April 3, 2018

**Abstract**

In this paper we propose and analyze an energy stable numerical scheme for the Cahn-Hilliard equation, with second order accuracy in time and the fourth order finite difference approximation in space. In particular, the truncation error for the long stencil fourth order finite difference approximation, over a uniform numerical grid with a periodic boundary condition, is analyzed, via the help of discrete Fourier analysis instead of the the standard Taylor expansion. This in turn results in a reduced regularity requirement for the test function. In the temporal approximation, we apply a second order BDF stencil, combined with a second order extrapolation formula applied to the concave diffusion term, as well as a second order artificial Douglas-Dupont regularization term, for the sake of energy stability. As a result, the unique solvability, energy stability are established for the proposed numerical scheme, and an optimal rate convergence analysis is derived in the $\ell^\infty(0,T;\ell^2)\cap\ell^2(0,T;H_h^2)$ norm. A few numerical experiments are presented, which confirm the robustness and accuracy of the proposed scheme.

**Key words.** Cahn-Hilliard equation, long stencil fourth order finite difference approximation, second order accuracy in time, energy stability, optimal rate convergence analysis, preconditioned steepest descent iteration

**AMS Subject Classification** 35K35, 35K55, 65K10, 65M06, 65M12

## 1 Introduction

In this article we consider an energy stable scheme for the Cahn-Hilliard equation, with second order temporal accuracy and long stencil fourth order finite difference spatial approximation. For any $\phi\in H^1(\Omega)$, with $\Omega\subset R^d$ ($d=2$ or $d=3$), the energy functional is given by (see [6] for a detailed derivation):

$$E(\phi)=\int_\Omega\left(\frac{1}{4}\phi^4-\frac{1}{2}\phi^2+\frac{1}{4}+\frac{\varepsilon^2}{2}|\nabla\phi|^2\right)d\mathbf{x}, \tag{1.1}$$

where the parmeter $\varepsilon$ controls the diffuse interface width. In turn, the Cahn-Hilliard equation is realized as the $H^{-1}$ conserved gradient flow of the energy functional (1.1):

$$\phi_t=\Delta\mu,\quad \mu:=\delta_\phi E=\phi^3-\phi-\varepsilon^2\Delta\phi, \tag{1.2}$$

*School of Science, Southwest University of Science and Technology, Mianyang, Sichuan 621010, P. R. China (zhengkelong@swust.edu.cn)

†Department of Mathematics, The University of Tennessee, Knoxville, TN 37996 (wfeng1@utk.edu)

‡Department of Mathematics, The University of Massachusetts, North Dartmouth, MA 02747 (Corresponding Author: cwang1@umassd.edu)

§Department of Mathematics, The University of Tennessee, Knoxville, TN 37996 (swise1@utk.edu)

where $\mu$ is the chemical potential and periodic boundary conditions are assumed. Subsequently, the energy dissipation law follows from an inner product with (1.2) by $\mu$: $E'(t) = -\int_\Omega |\nabla \mu|^2 d\mathbf{x} \le 0$. Meanwhile, because it is constructed as an $H^{-1}$ gradient flow, the equation is mass conservative: $\int_\Omega \partial_t \phi d\mathbf{x} = 0$.

The finite difference and finite element schemes to the CH equation have been extensively studied; see the related references [1, 16, 15, 22, 20, 28, 32, 37, 39, 43, 44, 45, 46, 63, 65], et cetera. Meanwhile, it is observed that, most finite difference works in the existing literature have been focused on the standard second order centered difference approximation; among the finite element works, most computations are based on either linear or quadratic polynomial elements. On the other hand, a fourth order and even more accurate spatial discretization is highly desirable, for the sake of its ability to capture the more detailed structure with a reduced computational cost. Of course, the spectral/pseudo-spectral approximation is one choice; see the related references [13, 48], etc. However, the spectral/pseudo-spectral differentiation turns out to be a global operator in space, and this feature leads to great challenges in the numerical implementations, especially in the case of an implicit treatment of nonlinear terms; and also, spectral/pseudo-spectral differentiation itself is involved with $O(N^d \ln N)$ float point calculations, instead of $O(N^d)$ scale for the finite difference ones.

This article is concerned with fourth order finite difference numerical approximation to the Cahn-Hilliard equation, with a theoretically justified energy stability and convergence. Among the existing fourth order finite difference works, it is worthy of mentioning [49], in which the authors considered a second order accurate in time, fourth order compact difference scheme. The error estimate was derived, while the energy stability has not been theoretically proved. Similar works could also be found in [47, 50, 58]. Meanwhile, we notice that, the compact difference approximation has always been involved with an additional discrete Poisson-like operator, therefore one more Poisson solver has to be included in the computational cost. Instead, if the long stencil fourth order finite difference is used in the numerical scheme, such an additional Poisson solver could be saved. In addition, the truncation error for the fourth order finite difference approximation, over a uniform numerical grid with a periodic boundary condition, is analyzed in this article. Instead of the classical maximum norm estimate for the truncation error, based on the standard Taylor expansion for the test function, we provide a discrete $\ell^2$ estimate. As a result, the regularity requirement is reduced to an $H^6$ bound for the test function, compared with the $C^6$ bound in the classical approach. In the 1-D case, such an estimate could be derived with an application of Taylor expansion in the integral form. In the 2-D and 3-D cases, the discrete and continuous Fourier expansions for the test function and its higher order derivatives are applied to obtain the discrete $\ell^2$ estimate for the truncation error, in which both the eigenvalue analysis and aliasing error control have to be considered.

In turn, we apply the long stencil fourth order difference discretization in space, combined with a second order accurate, energy stable temporal algorithm. There have been extensive studies on the second order (in time) energy stable numerical approach for the Cahn-Hilliard equation, based on the modified Crank-Nicolson version; see the related references [13, 15, 16, 17, 37, 38]. As an alternate numerical approach with energy stability, a careful numerical experiment in a recent finite element work [67] reveals that a modified backward differentiation formula (BDF) method could also preserve the desired energy stability for the Cahn-Hilliard flow. Furthermore, since the nonlinear term in the BDF method has a stronger convexity than the one in the Crank-Nicolson approach, a 20 to 25 percent improvement of the computational efficiency is generally expected. In addition, due to the long stencil operators involved in the fourth order spatial discretization, such an efficiency improvement is expected to be even more prominent. Consequently, we use the second order BDF concept to derive second order temporal accuracy, but modified so that the

concave diffusion term is treated explicitly. Such an explicit treatment for the concave part of the chemical potential ensures the unique solvability of the scheme without sacrificing energy stability. An additional term $A\Delta t\Delta(\phi^{k+1}-\phi^k)$ is added, which represents a second order Douglas-Dupont-type regularization, and a careful calculation shows that energy stability is guaranteed, provided a mild condition $A \geq \frac{1}{16}$ is enforced. As a result of this energy stability, a uniform in time $H^1$ bound for the numerical solution becomes available, with the discrete $H^1$ norm defined at an appropriate discrete level.

With such an $H_h^1$ bound at hand, we are able to derive a discrete $\ell^6$ bound for the numerical solution, uniform in time, with the help of discrete Sobolev embedding. Such an embedding analysis could be derived from a straightforward calculation; instead, a discrete Fourier analysis, combined with certain aliasing error estimate have to involved in the derivation. In turn, such an $\ell^6$ estimate enables one to obtain an optimal rate ($O(\Delta t^2+h^4)$) convergence analysis for the proposed numerical scheme, in the $\ell^\infty(0,T;\ell^2)\cap\ell^2(0,T;H_h^2)$ norm.

The outline of the paper is given as follows. In Section 2 we provide a discrete $\ell^2$ truncation error estimate for the long stencil fourth order finite difference approximation over a uniform numerical grid. The fully discrete scheme is formulated in Section 3, with the main theoretical results stated. The proof of these results is given by Section 4. The main numerical results are presented in Section 5. Finally, some concluding remarks are made in Section 6.

## 2 The long stencil difference operator and the local truncation error estimate

The long stencil fourth order finite difference formula can be derived by the Taylor expansion for the test function. In more detail, the fourth order approximations to the first and second order derivatives, over a uniform numerical grid, are given by

$$\mathcal{D}^1_{x,(4)} f_i = \tilde{D}_x(1-\frac{h^2}{6}D_x^2)f_i = \frac{f_{i-2}-8f_{i-1}+8f_{i+1}-f_{i+2}}{12h} = f'(x_i)+O(h^4), \tag{2.1}$$

$$\begin{aligned}\mathcal{D}^2_{x,(4)} f_i &= D_x^2(1-\frac{h^2}{12}D_x^2)f_i = \frac{-f_{i-2}+16f_{i-1}-30f_i+16f_{i+1}-f_{i+2}}{12h^2}\\ &= f''(x_i)+O(h^4),\end{aligned} \tag{2.2}$$

where $\tilde{D}_x$ and $D_x^2$ are the standard centered difference approximation to the first and second order derivatives, respectively. See the detailed derivations in the related references [30, 31, 42, 55], etc. These long stencil fourth order finite difference approximations have been extensively applied to different types of partial differential equations (PDEs), such as incompressible Boussinesq equation [53, 60], three-dimensional geophysical fluid models [52, 56], the Maxwell equation [25].

In the consistency analysis for these long stencil fourth order finite difference schemes, we denote a continuous function $f$, with certain regularity assumption, to be the test function to demonstrate the accuracy order of the difference operators. Note that the concept of such a test function is different from the corresponding notation in the finite element method. The classical truncation error estimate implies that

$$\|\tau_1\|_\infty \leq Ch^4\|f\|_{C^5}, \quad \text{with } (\tau_1)_i = \mathcal{D}^1_{x,(4)}f_i - f'(x_i), \tag{2.3}$$

$$\|\tau_2\|_\infty \leq Ch^4\|f\|_{C^6}, \quad \text{with } (\tau_2)_i = \mathcal{D}^2_{x,(4)}f_i - f''(x_i), \tag{2.4}$$

in which the $C^m$ regularity of the test function is involved. Meanwhile, for most time-dependent PDEs, a max-norm bound of the truncation error (in the $\|\cdot\|_\infty$ norm) is not necessary in the

numerical analysis. Indeed, a discrete $\ell^2$ bound of the truncation error is typically sufficient in the convergence analysis. Subsequently, a natural question arises: could a discrete $\ell^2$ estimate be available for the truncation error associated with the fourth order finite difference approximation, which only requires an $H^m$ regularity for the test function?

This important issue is studied in this section. We begin with the analysis for the 1-D case.

## 2.1 A discrete $\ell^2$ truncation error estimate over a 1-D numerical grid

Consider a 1-D domain $\Omega = (0, L)$, a uniform grid $x_i = ih$, with $h = L/N^*$, $0 \le i \le N^* - 1$. For any discrete grid function $g$, which is evaluated at grid points $x_i$, $0 \le i \le N^* - 1$, the discrete $\ell^2$ norm is introduced as

$$\|g\|_2^2 = h \sum_{i=0}^{N^*-1} g_i^2. \tag{2.5}$$

**Proposition 2.1.** *For $f \in H^6_{per}(\Omega) := \{f \in H^6(\Omega) : f \text{ is periodic}\}$, we have*

$$\|\tau\|_2 \le Ch^4 \|f\|_{H^6}, \quad \text{with } \tau_i = \mathcal{D}^2_{x,(4)} f_i - f''(x_i), \tag{2.6}$$

*in which the fourth order finite difference operator $\mathcal{D}^2_{x,(4)}$ is given by (2.4).*

*Proof.* An application of Taylor's series in integral form shows that

$$\begin{aligned}
f_{i+1} &= f_i + hf'(x_i) + \frac{h^2}{2} f''(x_i) + \frac{h^3}{6} f'''(x_i) + \frac{h^4}{24} f^{(4)}(x_i) + \frac{h^5}{120} f^{(5)}(x_i) \\
&\quad + \int_{x_i}^{x_{i+1}} \frac{f^{(6)}(t)}{120} (x_{i+1} - t)^5 dt, \qquad (2.7) \\
f_{i-1} &= f_i - hf'(x_i) + \frac{h^2}{2} f''(x_i) - \frac{h^3}{6} f'''(x_i) + \frac{h^4}{24} f^{(4)}(x_i) - \frac{h^5}{120} f^{(5)}(x_i) \\
&\quad + \int_{x_i}^{x_{i-1}} \frac{f^{(6)}(t)}{120} (x_{i-1} - t)^5 dt, \qquad (2.8) \\
f_{i+2} &= f_i + 2hf'(x_i) + \frac{4h^2}{2} f''(x_i) + \frac{8h^3}{6} f'''(x_i) + \frac{16h^4}{24} f^{(4)}(x_i) + \frac{32h^5}{120} f^{(5)}(x_i) \\
&\quad + \int_{x_i}^{x_{i+2}} \frac{f^{(6)}(t)}{120} (x_{i+2} - t)^5 dt, \qquad (2.9) \\
f_{i-2} &= f_i - 2hf'(x_i) + \frac{4h^2}{2} f''(x_i) - \frac{8h^3}{6} f'''(x_i) + \frac{16h^4}{24} f^{(4)}(x_i) - \frac{32h^5}{120} f^{(5)}(x_i) \\
&\quad + \int_{x_i}^{x_{i-2}} \frac{f^{(6)}(t)}{120} (x_{i-2} - t)^5 dt. \qquad (2.10)
\end{aligned}$$

These expansions in turn yield that

$$\begin{aligned}
\tau_i = \mathcal{D}^2_{x,(4)} f_i - f''(x_i) &= \frac{-f_{i-2} + 16f_{i-1} - 30f_i + 16f_{i+1} - f_{i+2}}{12h^2} - f''(x_i) \\
&= \frac{1}{1440h^2} \Big( 16 \int_{x_i}^{x_{i+1}} f^{(6)}(t)(x_{i+1} - t)^5 dt - 16 \int_{x_{i-1}}^{x_i} f^{(6)}(t)(x_{i-1} - t)^5 dt \\
&\quad - \int_{x_i}^{x_{i+2}} f^{(6)}(t)(x_{i+2} - t)^5 dt + \int_{x_{i-2}}^{x_i} f^{(6)}(t)(x_{i-2} - t)^5 dt \Big). \qquad (2.11)
\end{aligned}$$

Meanwhile, an application of Hölder's inequality implies that

$$\begin{aligned}
&\left|\int_{x_i}^{x_{i+1}} f^{(6)}(t)(x_{i+1}-t)^5 dt\right| \\
\leq\ & \left\|f^{(6)}(t)\right\|_{\ell^2(x_i,x_{i+1})} \cdot \left\|(x_{i+1}-t)^5\right\|_{\ell^2(x_i,x_{i+1})} = \frac{1}{\sqrt{11}} h^{11/2} \left\|f^{(6)}(t)\right\|_{\ell^2(x_i,x_{i+1})}, \qquad (2.12)\\
&\left|\int_{x_{i-1}}^{x_i} f^{(6)}(t)(x_{i-1}-t)^5 dt\right| \leq \frac{1}{\sqrt{11}} h^{11/2} \left\|f^{(6)}(t)\right\|_{\ell^2(x_{i-1},x_i)}, \qquad (2.13)\\
&\left|\int_{x_i}^{x_{i+2}} f^{(6)}(t)(x_{i+2}-t)^5 dt\right| \leq \frac{32\sqrt{2}}{\sqrt{11}} h^{11/2} \left\|f^{(6)}(t)\right\|_{\ell^2(x_i,x_{i+2})}, \qquad (2.14)\\
&\left|\int_{x_{i-2}}^{x_i} f^{(6)}(t)(x_{i-2}-t)^5 dt\right| \leq \frac{32\sqrt{2}}{\sqrt{11}} h^{11/2} \left\|f^{(6)}(t)\right\|_{\ell^2(x_{i-2},x_i)}. \qquad (2.15)
\end{aligned}$$

Its combination with (2.11) leads to

$$|\tau_i| \leq \frac{1+2\sqrt{2}}{45\sqrt{11}} h^{7/2} \left\|f^{(6)}(t)\right\|_{\ell^2(x_{i-2},x_{i+2})}. \qquad (2.16)$$

In turn, a discrete $\ell^2$ estimate of the truncation error $\tau$ is obtained:

$$\begin{aligned}
&h \sum_{i=0}^{N^*-1} |\tau_i|^2 \leq Ch^8 \sum_{i=0}^{N^*-1} \left\|f^{(6)}(t)\right\|^2_{\ell^2(x_{i-2},x_{i+2})} \leq 4Ch^8 \left\|f^{(6)}(t)\right\|^2_{\ell^2(0,L)},\\
&\text{i.e.} \quad \|\tau\|_2 \leq Ch^4 \|f\|_{H^6(0,L)}, \qquad (2.17)
\end{aligned}$$

in which the second step comes from the following obvious fact:

$$\sum_{i=0}^{N^*-1} \left\|f^{(6)}(t)\right\|^2_{\ell^2(x_{i-2},x_{i+2})} \leq 4 \left\|f^{(6)}(t)\right\|^2_{\ell^2(0,L)}. \qquad (2.18)$$

Proposition 2.1 is proven. □

**Remark 2.2.** *A detailed calculation reveals that the standard Taylor expansion results in the classical truncation error estimate as (2.4), with a $C^6$ regularity requirement for the test function; while the Taylor expansion in the integral form gives an improved truncation error estimate (2.6), in which only an $H^6$ regularity requirement is set for the test function.*

**Remark 2.3.** *For the long stencil fourth order finite difference approximation (2.1) to the first order derivative, the following discrete $\ell^2$ truncation error estimate can be derived in a similar manner:*

$$\|\tau_1\|_2 \leq Ch^4 \|f\|_{H^5}, \quad \textit{with } (\tau_1)_i = \mathcal{D}^1_{x,(4)} f_i - f'(x_i). \qquad (2.19)$$

*The details are skipped for brevity.*

## 2.2 The 2-D and 3-D analyses

Consider a 2-D domain $\Omega = (0, L)^2$ with a uniform grid $(x_i, y_j) = (ih, jh)$, $h = L/N^*$, $0 \leq i, j \leq 2N$, and periodic boundary conditions in both directions. For simplicity of presentation in the Fourier

analysis, it is assumed that $N^* = 2N + 1$. We also make a 2-D extension of the fourth order long stencil finite difference operator as $\Delta_{h,(4)} = \mathcal{D}^2_{x,(4)} + D^2_{y,(4)}$:

$$\mathcal{D}^2_{x,(4)} f_{i,j} = D_x^2(1 - \frac{h^2}{12} D_x^2) f_{i,j} = \frac{-f_{i-2,j} + 16 f_{i-1,j} - 30 f_{i,j} + 16 f_{i+1,j} - f_{i+2,j}}{12h^2}, \tag{2.20}$$

$$\mathcal{D}^2_{y,(4)} f_{i,j} = D_y^2(1 - \frac{h^2}{12} D_y^2) f_{i,j} = \frac{-f_{i,j-2} + 16 f_{i,j-1} - 30 f_{i,j} + 16 f_{i,j+1} - f_{i,j+2}}{12h^2}. \tag{2.21}$$

In addition, for any discrete grid function $g$, which is evaluated at 2-D grid points $(x_i, y_j)$, $0 \le i, j \le N^* - 1$, the discrete $\ell^2$ norm is defined as

$$\|g\|_2^2 = h^2 \sum_{i,j=0}^{N^*-1} g_{i,j}^2. \tag{2.22}$$

**Proposition 2.4.** *For $f \in H^6_{per}(\Omega)$, we have*

$$\|\tau\|_2 \le C h^4 \|f\|_{H^6}, \quad \text{with } \tau_{i,j} = \Delta_{h,(4)} f_{i,j} - (\Delta f)(x_i, y_j), \tag{2.23}$$

*in which $C$ only depends on $L$.*

**Remark 2.5.** *Other than the long stencil difference operator* (2.2)*, the compact fourth order difference approximations have also been widely studied in the existing literature [47, 50, 58]*

$$\Delta = \frac{\Delta_h + \frac{h^2}{6} D_x^2 D_y^2}{1 + \frac{h^2}{12}\Delta_h} + O(h^4), \tag{2.24}$$

*which comes from a standard Taylor expansion:*

$$(\Delta_h + \frac{h^2}{6} D_x^2 D_y^2) f = \Delta f + \frac{h^2}{12}\Delta^2 f + O(h^4). \tag{2.25}$$

*On the other hand, whenever a time-dependent problem is considered, with $\Delta f = g$, one has to denote an intermediate variable $\overline{g} = (1 + \frac{h^2}{12}\Delta_h) g$ at the numerical grid. In turn, two Poisson-like equations have to be solved at the numerical level: $(\Delta_h + \frac{h^2}{6} D_x^2 D_y^2) f = \overline{g}$ to obtain $f$, and $(1 + \frac{h^2}{12}\Delta_h) g = \overline{g}$ to obtain $g$, since both $f$ and $g$ are usually involved in the original PDE, in particular for the nonlinear problems. In contrast, for the the long stencil difference operator* (2.2)*, we only need to solve one Poisson-like equation $(\mathcal{D}^2_{x,(4)} + \mathcal{D}^2_{y,(4)}) f = g$. And also, this equation could be very efficiently solved via an FFT-based fact algorithm, since the long-stencil difference operator shares exact the same eigenvectors as the standard Laplacian operator $\Delta_h$, with only a minor modification in the corresponding eigenvalues.*

## 2.3 Review of Fourier series and interpolation

For $f(x, y) \in L^2(\Omega)$, $\Omega = (0, L)^2$, with Fourier series

$$f(x, y) = \sum_{k,l=-\infty}^{\infty} \hat{f}_{k,l} \mathrm{e}^{2\pi \mathrm{i}(kx+ly)/L}, \quad \text{with} \quad \hat{f}_{k,l} = \int_\Omega f(x, y) \mathrm{e}^{-2\pi \mathrm{i}(kx+ly)/L} dxdy, \tag{2.26}$$

its truncated series is defined as the projection onto the space $\mathcal{B}^N$ of trigonometric polynomials in $x$ and $y$ of degree up to $N$, given by

$$\mathcal{P}_N f(x, y) = \sum_{k,l=-N}^{N} \hat{f}_{k,l} \mathrm{e}^{2\pi \mathrm{i}(kx+ly)/L}. \tag{2.27}$$

Meanwhile, an interpolation operator $\mathcal{I}_N$ is introduced if one wants an approximation which matches the function at a given set of points. Given a uniform numerical grid with $(2N+1)$ points in each dimension and a grid function $\mathbf{f}$, where $\mathbf{f}_{i,j} = f(x_i, y_j)$, the Fourier interpolation of the function is defined by

$$\mathcal{I}_N f(x,y) = \sum_{k,l=-N}^{N} (\hat{f}_c^N)_{k,l} \mathrm{e}^{2\pi \mathrm{i}(kx+ly)/L}, \tag{2.28}$$

where the $(2N+1)^2$ pseudospectral coefficients $(\hat{f}_c^N)_{k,l}$ are be computed based on the interpolation requirement

$$f(x_i, y_j) = \mathcal{I}_N f(x_i, y_j)$$

at the $(2N+1)^2$ equidistant points [5, 33, 40]. Note that these *collocation* coefficients can be efficiently computed using the fast Fourier transform (FFT). Also, observe that these interpolation coefficients are not equal to the actual Fourier coefficients. The difference between them is known as the aliasing error. In general, $\mathcal{P}_N f(x,y) \neq \mathcal{I}_N f(x,y)$, and even $\mathcal{P}_N f(x_i, y_j) \neq \mathcal{I}_N f(x_i, y_j)$, except of course in the case that $f \in \mathcal{B}^N$.

The consistency and accuracy of the Fourier projection and interpolation have been well established in the existing literature. As long as $f \in H^m_{per}(\Omega)$, the convergence of the derivatives of the projection and interpolation is given by

$$\begin{aligned} \|\partial^\alpha f - \partial^\alpha \mathcal{P}_N f\| &\leq C\|f^{(m)}\| h^{m-|\alpha|}, \quad \text{for } 0 \leq |\alpha| \leq m, \\ \|\partial^\alpha f - \partial^\alpha \mathcal{I}_N f\| &\leq C\|f\|_{H^m} h^{m-|\alpha|}, \quad \text{for } 0 \leq |\alpha| \leq m,\ m > \frac{d}{2}, \end{aligned} \tag{2.29}$$

where $\|\cdot\|$ denotes the standard $\ell^2$ norm and $d$ is the dimension. For more details, see the discussion of approximation theory by Canuto and Quarteroni [7] .

## 2.4 Proof of Proposition 2.4

Assume that $f \in H^6_{per}$ has a Fourier expansion

$$f(x,y) = \sum_{k,l=-\infty}^{\infty} \hat{f}_{k,l} \exp\left(2\pi \mathrm{i}(kx+ly)/L\right). \tag{2.30}$$

The Parseval equality shows that

$$\|f\|_2^2 = L^2 \sum_{k,l=-\infty}^{\infty} \left|\hat{f}_{k,l}\right|^2. \tag{2.31}$$

Similarly, for the derivatives, we have

$$\Delta^{m_0} f(x,y) = \sum_{k,l=-\infty}^{\infty} \left(-(\frac{2\pi}{L})^2 (k^2+l^2)\right)^{m_0} \hat{f}_{k,l} \exp\left(2\pi \mathrm{i}(kx+ly)/L\right), \tag{2.32}$$

for $m_0 \geq 1$, and the corresponding Parseval equality gives

$$\|\Delta^{m_0} f\|_2^2 = L^2 \sum_{k,l=-\infty}^{\infty} \left(\frac{4\pi^2}{L^2}(k^2+l^2)\right)^{2m_0} \left|\hat{f}_{k,l}\right|^2. \tag{2.33}$$

In particular, we see that

$$\begin{aligned} \|\Delta f\|_2^2 &= L^2 \sum_{k,l=-\infty}^{\infty} \left(\frac{4\pi^2}{L^2}(k^2+l^2)\right)^2 \left|\hat{f}_{k,l}\right|^2, \\ \left\|\Delta^3 f\right\|_2^2 &= L^2 \sum_{k,l=-\infty}^{\infty} \left(\frac{4\pi^2}{L^2}(k^2+l^2)\right)^6 \left|\hat{f}_{k,l}\right|^2. \end{aligned} \tag{2.34}$$

We also note that for any (periodic) discrete grid function over $(x_i, y_j)$, $0 \le i, j \le 2N$, with a discrete Fourier expansion

$$g_{i,j} = \sum_{k,l=-N}^{N} \hat{g}_{k,l} \exp\left(2\pi \mathrm{i}(kx_i + ly_j)/L\right), \tag{2.35}$$

the corresponding discrete Parseval equality is valid:

$$h^2 \sum_{i,j=0}^{2N} |g_{i,j}|^2 = L^2 \sum_{k,l=-N}^{N} |\hat{g}_{k,l}|^2. \tag{2.36}$$

Meanwhile, we observe that the discrete Fourier expansion of $f$ over the uniform grid $(x_i, y_j)$, $0 \le i, j \le 2N$, is not the projection of (2.30), due to the appearance of aliasing errors. A more careful calculation reveals that

$$f_{i,j} = \sum_{k,l=-N}^{N} \tilde{\hat{f}}_{k,l} \exp\left(2\pi \mathrm{i}(kx_i + ly_j)/L\right), \quad \text{with } \tilde{\hat{f}}_{k,l} = \sum_{k_1,l_1=-\infty}^{\infty} \hat{f}_{k+k_1N^*, l+l_1N^*}. \tag{2.37}$$

(See the related derivations in [59].) In turn, taking the centered difference $\mathcal{D}^2_{x,(4)}$, $\mathcal{D}^2_{y,(4)}$ on $f$ and making use of the fact that $\exp\left(2\pi \mathrm{i}(kx_i + ly_j)/L\right)$ is also an eigenfunction of the discrete operator $\Delta_{h,(4)}$ lead to the following formulas:

$$\Delta_{h,(4)} f_{i,j} = \sum_{k,l=-N}^{N} \left(\lambda_{kx,(4)} + \lambda_{ly,(4)}\right) \tilde{\hat{f}}_{k,l} \exp\left(2\pi \mathrm{i}(kx_i + ly_j)/L\right), \tag{2.38}$$

where

$$\lambda_{kx,(4)} = \lambda_k - \frac{h^2}{12}\lambda_k^2, \ \lambda_{ly,(4)} = \lambda_l - \frac{h^2}{12}\lambda_l^2, \ \lambda_k = \frac{-4\sin^2(k\pi h/L)}{h^2}, \quad \lambda_l = \frac{-4\sin^2(l\pi h/L)}{h^2}. \tag{2.39}$$

Moreover, a differentiation of the Fourier expansion (2.30) leads to

$$\Delta f(x,y) = \sum_{k,l=-\infty}^{\infty} \left(\frac{-4\pi^2}{L^2}(k^2+l^2)\right) \hat{f}_{k,l} \exp\left(2\pi \mathrm{i}(kx + ly)/L\right), \tag{2.40}$$

and its interpolation at $(x_i, y_j)$ gives

$$(\Delta f)_{i,j} = \sum_{k,l=-N}^{N} \tilde{\hat{f}}^{(2)}_{k,l} \exp\left(2\pi \mathrm{i}(kx_i + ly_j)/L\right), \tag{2.41}$$

with

$$\tilde{\hat{f}}^{(2)}_{k,l} = \sum_{k_1,l_1=-\infty}^{\infty} \left( \frac{-4(k+k_1N^*)^2\pi^2 - 4(l+l_1N^*)^2\pi^2}{L^2} \right) \hat{f}_{k+k_1N^*,l+l_1N^*}. \tag{2.42}$$

Therefore, the difference between (2.38) and (2.42) gives

$$\tau_{i,j} = \sum_{k=-N}^{N} \left( \left( \lambda_{kx,(4)} + \lambda_{ly,(4)} \right) \tilde{\hat{f}}_{k,l} - \tilde{\hat{f}}^{(2)}_{k,l} \right) \exp\left( 2\pi \mathrm{i}(kx_i + ly_j)/L \right). \tag{2.43}$$

As a result, an application of discrete Parseval equality yields

$$\|\tau\|_2^2 = L^2 \sum_{k,l=-N}^{N} \left| \left( \lambda_{kx,(4)} + \lambda_{ly,(4)} \right) \tilde{\hat{f}}_{k,l} - \tilde{\hat{f}}^{(2)}_{k,l} \right|^2. \tag{2.44}$$

Moreover, a detailed comparison between (2.37) and (2.42) results in

$$\begin{aligned} \left( \lambda_{kx,(4)} + \lambda_{ly,(4)} \right) \tilde{\hat{f}}_{k,l} - \tilde{\hat{f}}^{(2)}_{k,l} \quad &= \quad \left( \left( \lambda_{kx,(4)} + \frac{4k^2\pi^2}{L^2} \right) + \left( \lambda_{ly,(4)} + \frac{4l^2\pi^2}{L^2} \right) \right) \hat{f}_{k,l} \\ &+ \sum_{\substack{k_1,l_1=-\infty \\ (k_1,l_1)\neq(0,0)}}^{\infty} \left\{ \left( \lambda_{kx,(4)} + \frac{4(k+k_1N^*)^2\pi^2}{L^2} \right) \right. \\ &\left. + \left( \lambda_{ly,(4)} + \frac{4(l+l_1N^*)^2\pi^2}{L^2} \right) \right\} \hat{f}_{k+k_1N^*,l+l_1N^*}. \end{aligned} \tag{2.45}$$

The estimates of the above terms are given by the following lemmas. The proofs will be provided in the appendix.

**Lemma 2.6.** *We have, for some $C_1 > 0$,*

$$\left| \lambda_{kx,(4)} + \frac{4k^2\pi^2}{L^2} \right| \le C_1 h^4 \left( \frac{2k\pi}{L} \right)^6, \quad \left| \lambda_{ly,(4)} + \frac{4l^2\pi^2}{L^2} \right| \le C_1 h^4 \left( \frac{2l\pi}{L} \right)^6, \quad \forall\ 0 \le k,l \le N. \tag{2.46}$$

**Lemma 2.7.** *We have*

$$\begin{aligned} \sum_{k,l=-N}^{N} \left| \sum_{\substack{k_1,l_1=-\infty \\ (k_1,l_1)\neq(0,0)}}^{\infty} \left( \lambda_{kx,(4)} + \frac{4(k+k_1N^*)^2\pi^2}{L^2} \right) \hat{f}_{k+k_1N^*,l+l_1N^*} \right|^2 &\le C_2 h^8 \|f\|^2_{H^6}, \\ \sum_{k,l=-N}^{N} \left| \sum_{\substack{k_1,l_1=-\infty \\ (k_1,l_1)\neq(0,0)}}^{\infty} \left( \lambda_{ly,(4)} + \frac{4(l+l_1N^*)^2\pi^2}{L^2} \right) \hat{f}_{k+k_1N^*,l+l_1N^*} \right|^2 &\le C_2 h^8 \|f\|^2_{H^6}, \end{aligned} \tag{2.47}$$

*where $C_2 > 0$ is a constant that only depends on $L$.*

A direct consequence of Lemma 2.6 shows that

$$\begin{aligned} \sum_{k,l=-N}^{N} \left( \lambda_{kx,(4)} + \frac{4k^2\pi^2}{L^2} \right)^2 \left| \hat{f}_{k,l} \right|^2 \le \sum_{k,l=-N}^{N} C_1^2 h^8 \left( \frac{2k\pi}{L} \right)^{12} \left| \hat{f}_{k,l} \right|^2 \le \tilde{C}_1 h^8 \|f\|^2_{H^6}, \\ \sum_{k,l=-N}^{N} \left( \lambda_{ly,(4)} + \frac{4l^2\pi^2}{L^2} \right)^2 \left| \hat{f}_{k,l} \right|^2 \le \sum_{k,l=-N}^{N} C_1^2 h^8 \left( \frac{2l\pi}{L} \right)^{12} \left| \hat{f}_{k,l} \right|^2 \le \tilde{C}_1 h^8 \|f\|^2_{H^6}, \end{aligned} \tag{2.48}$$

with $\tilde{C}_1 = \frac{C_1^2}{L^2}$, in which we used the estimate (2.34)

$$\sum_{k,l=-N}^{N} \left( \left(\frac{2k\pi}{L}\right)^{12} + \left(\frac{2l\pi}{L}\right)^{12} \right) \left|\hat{f}_{k,l}\right|^2 \leq \sum_{k,l=-\infty}^{\infty} \left( \left(\frac{2k\pi}{L}\right)^{12} + \left(\frac{2l\pi}{L}\right)^{12} \right) \left|\hat{f}_{k,l}\right|^2 \leq \frac{1}{L^2} \left\|\Delta^3 f\right\|^2. \tag{2.49}$$

A combination of (2.45), (2.48) and Lemma 2.7 indicates that

$$\begin{aligned}
&\sum_{k,l=-N}^{N} \left| \left(\lambda_{kx,(4)} + \lambda_{ly,(4)}\right) \tilde{\hat{f}}_{k,l} - \tilde{\hat{f}}^{(2)}_{k,l} \right|^2 \\
&\qquad \leq \; 4 \sum_{k,l=-N}^{N} \Bigg\{ \left( \left(\lambda_{kx,(4)} + \frac{4k^2\pi^2}{L^2}\right)^2 + \left(\lambda_{ly,(4)} + \frac{4l^2\pi^2}{L^2}\right)^2 \right) \left|\hat{f}_{k,l}\right|^2 \\
&\qquad\quad + \left| \sum_{\substack{k_1,l_1=-\infty \\ (k_1,l_1)\neq(0,0)}}^{\infty} \left(\lambda_{kx,(4)} + \frac{4(k+k_1N^*)^2\pi^2}{L^2}\right) \hat{f}_{k+k_1N^*,l+l_1N^*} \right|^2 \\
&\qquad\quad + \left| \sum_{\substack{k_1,l_1=-\infty \\ (k_1,l_1)\neq(0,0)}}^{\infty} \left(\lambda_{ly,(4)} + \frac{4(l+l_1N^*)^2\pi^2}{L^2}\right) \hat{f}_{k+k_1N^*,l+l_1N^*} \right|^2 \Bigg\} \\
&\qquad \leq \; \tilde{C}_2 h^8 \left\|f\right\|^2_{H^6},
\end{aligned} \tag{2.50}$$

where $\tilde{C}_2 = 8\tilde{C}_1 + 8C_2$. Observe that the Cauchy inequality

$$|a_1 + a_2 + a_3 + a_4|^2 \leq 4(|a_1|^2 + |a_2|^2 + |a_3|^2 + |a_4|^2)$$

was applied in the first step.

Finally, a substitution of (2.50) into (2.44) results in (2.23), with the constant $C$ given by

$$C = \sqrt{\tilde{C}_2} L. \tag{2.51}$$

This completes the proof of Proposition 2.4.

## 2.5 An extension to a 3-D domain

Similarly, consider a 3-D domain $\Omega = (0, L)^3$ with a uniform grid $(x_i, y_j, z_k) = (ih, jh, kh)$, $h = L/N^*$, $(N^* = 2N + 1)$, $0 \leq i, j, k \leq 2N$, and periodic boundary conditions in both $x$, $y$ and $z$ directions. The 3-D extension of the fourth order long stencil finite difference operator as $\Delta_{h,(4)} = \mathcal{D}^2_{x,(4)} + D^2_{y,(4)} + D^2_{z,(4)}$ can be defined in the same way as (2.20)-(2.21). For any 3-D discrete grid function $g$, at grid points $(x_i, y_j, z_k)$, $0 \leq i, j, k \leq N^* - 1$, the discrete $\ell^2$ norm is given by

$$\|g\|_2 = \left( h^3 \sum_{i,j,k=0}^{N^*-1} g^2_{i,j,k} \right)^{\frac{1}{2}}. \tag{2.52}$$

The discrete $\ell^2$ truncation error estimate can be performed in a similar fashion as in the 2-D case. Both the continuous Fourier expansion for the test function and the discrete expansions of its higher order derivatives interpolated at the numerical grid points have to be analyzed. Lemma

2.6 is still valid, which provides a detailed eigenvalue comparison and analysis between $\Delta_{h,(4)}$ and $\Delta$. Furthermore, Lemma 2.7 can be established in a similar way, and the convergence property of the following triple series plays a key role:

$$\sum_{\substack{k_1,l_1,m1=-\infty \\ (k_1,l_1,m1)\neq(0,0,0)}}^{\infty} \frac{1}{\left((|k_1|-\frac{1}{2})^2+(|l_1|-\frac{1}{2})^2+(|m_1|-\frac{1}{2})^2\right)^{\beta_0}}, \tag{2.53}$$

with $\beta_0 = 2$ is convergent, where $\beta_0 = \frac{K_0}{2} = 2$, with the accuracy order $K_0 = 4$.

As a result, the following theorem could be established. Its detailed proof is skipped for brevity.

**Proposition 2.8.** *For $f \in H^6_{per}(\Omega)$, with $\Omega = (0, L)^3$, we have*

$$\|\tau\|_2 \le Ch^4 \|f\|_{H^6}, \quad \text{with } \tau_{i,j,k} = \Delta_{h,(4)} f_{i,j,k} - (\Delta f)(x_i, y_j, z_k), \tag{2.54}$$

*in which $C$ only depends on $L$.*

**Remark 2.9.** *For simplicity of presentation, we use periodic boundary condition for the test function and its discrete version. On the other hand, if other type physical boundary conditions, such as homogeneous Neumann boundary condition is considered, the corresponding analysis for the long stencil difference approximation* (2.1), (2.2)*, could be derived in the same manner, under the assumption of the same Neumann boundary condition for its Laplacian operator. Such an assumption is valid in many physically interesting phase field models, such as the Cahn-Hilliard equation in the next section. The details of these estimates will be left in the future works.*

# 3 The numerical scheme for the Cahn-Hilliard equation

For simplicity, we focus our attention on a 2-D domain. The extension to the 3-D case is expected to be straightforward.

## 3.1 The spatial discretization and the related notations

As defined in the previous section, it is assumed that assume $\Omega = (0, L)^2$. We write $L = m \cdot h$, where $m$ is a positive integer. The parameter $h = \frac{L}{m}$ is called the mesh or grid spacing. We define the following uniform, infinite grid with grid spacing $h > 0$: $E := \{x_i \mid i \in \mathbb{Z}\}$, with $x_i := (i - \frac{1}{2})h$. Consider the following 2-D discrete periodic function spaces:

$$\mathcal{V}_{\rm per} := \{\nu : E \times E \to \mathbb{R} \mid \nu_{i,j} = \nu_{i+\alpha m, j+\beta m},\ \forall\, i, j, \alpha, \beta \in \mathbb{Z}\}.$$

We also define the mean zero space

$$\mathring{\mathcal{V}}_{\rm per} := \left\{ \nu \in \mathcal{V}_{\rm per} \,\middle|\, \overline{\nu} := \frac{h^2}{|\Omega|} \sum_{i,j=1}^{m} \nu_{i,j} = 0 \right\}.$$

The 4th order 2-D discrete Laplacian, $\Delta_{h,(4)} : \mathcal{V}_{\rm per} \to \mathcal{V}_{\rm per}$, is given by

$$\Delta_{h,(4)} := \mathcal{D}^2_{x,(4)} + D^2_{y,(4)}.$$

Now we define the following discrete inner products:

$$(\nu, \xi)_2 := h^2 \textstyle\sum_{i,j=1}^{m} \nu_{i,j}\psi_{i,j}, \quad \nu,\, \xi \in \mathcal{V}_{\rm per}.$$

Suppose that $\zeta \in \mathring{\mathcal{V}}_{\rm per}$, then there is a unique solution $\mathsf{T}_h[\zeta] \in \mathring{\mathcal{V}}_{\rm per}$ such that $-\Delta_{h,(4)}\mathsf{T}_h[\zeta] = \zeta$. We often write, in this case, $\mathsf{T}_h[\zeta] = -\Delta_{h,(4)}^{-1}\zeta$. The discrete analog of the $\mathring{H}_{\rm per}^{-1}$ inner product is defined as

$$(\zeta, \xi)_{-1} := (\zeta, \mathsf{T}_h[\xi])_2 = (\mathsf{T}_h[\zeta], \xi)_2\,, \quad \zeta,\, \xi \in \mathring{\mathcal{V}}_{\rm per}.$$

With the above machinery, if $\nu \in \mathring{\mathcal{V}}_{\rm per}$, then $\|\nu\|_{-1,h}^2 = (\nu,\nu)_{-1}$. If $\nu \in \mathcal{V}_{\rm per}$, then $\|\nu\|_2^2 := (\nu,\nu)_2$; $\|\nu\|_p^p := (|\nu|^p, 1)_2$ $(1 \le p < \infty)$, and $\|\nu\|_\infty := \max_{\substack{1\le i\le m\\ 1\le j\le n}} |\nu_{i,j}|$.

For $\phi, \psi \in \mathring{\mathcal{V}}_{\rm per}$, the following summation by parts formulas are available:

$$-(\phi, \Delta_{h,(4)}\psi)_2 = -(\Delta_{h,(4)}\phi, \psi)_2 = (\nabla_h\phi, \nabla_h\psi)_2 + \frac{h^2}{12}(\Delta_h\phi, \Delta_h\psi)_2, \tag{3.1}$$

$$(\mathsf{T}_h\phi, (-\Delta_{h,(4)})\psi)_2 = (\phi, \psi)_2. \tag{3.2}$$

In turn, we denote the following norm for the discrete gradient, corresponding to the long stencil difference:

$$\|\nabla_{h,(4)} f\|_2^2 = \|\nabla_h f\|_2^2 + \frac{h^2}{12}\|\Delta_h f\|_2^2. \tag{3.3}$$

In addition, the discrete $\|\cdot\|_{H_h^1}$ and $\|\cdot\|_{H_h^2}$ norms are given by

$$\|f\|_{H_h^1}^2 := \|f\|_2^2 + \|\nabla_h f\|_2^2\,, \quad \|f\|_{H_h^2}^2 := \|f\|_{H_h^1}^2 + \|\Delta_h\phi\|_2^2\,. \tag{3.4}$$

For any periodic grid function $\phi$, the discrete energy is introduced as

$$E_h(\phi) = \frac{1}{4}\|\phi\|_4^4 - \frac{1}{2}\|\phi\|_2^2 + \frac{1}{4}|\Omega| + \frac{\varepsilon^2}{2}\|\nabla_{h,(4)}\phi\|_2^2, \tag{3.5}$$

The following result, a discrete Sobolev embedding from $H_h^1$ to $\ell^6$, could be derived in the same manner as Lemma 2.1 in [13], and Lemma 5.1 in [26]. The details are left to interested readers; also see the related analyses in [27].

**Lemma 3.1.** *For any periodic grid function $f$, we have*

$$\|f\|_6 \le C(\|f\|_2 + \|\nabla_h f\|_2), \tag{3.6}$$

*for some constant $C$ only dependent on $\Omega$.*

The inequalities in the next lemma will play an important role in the energy stability and optimal rate convergence analysis. A direct calculation is not able to derive these inequalities; instead, a discrete Fourier analysis has to be applied in the derivation; the details will be left in Appendix A.

**Lemma 3.2.** *We have*

$$\|f\|_2^2 \le \|f\|_{-1,h} \cdot \|\nabla_{h,(4)} f\|_2, \quad \forall f \in \mathring{\mathcal{V}}_{\rm per}, \tag{3.7}$$

$$\|\Delta_h f\|_2 \le \|\Delta_{h,(4)} f\|_2, \quad \forall f \in \mathcal{V}_{\rm per}. \tag{3.8}$$

### 3.2 The fully discrete scheme and the main theoretical results

A modified second order BDF temporal discretization is applied to the Cahn-Hilliard equation, combined with long stencil fourth order difference approximation in space:

$$\frac{\frac{3}{2}\phi^{k+1} - 2\phi^k + \frac{1}{2}\phi^{k-1}}{\Delta t} = \Delta_{h,(4)}\mu_h^{k+1}, \tag{3.9}$$

$$\mu_h^{k+1} = (\phi^{k+1})^3 - 2\phi^k + \phi^{k-1} - \varepsilon^2\Delta_{h,(4)}\phi^{k+1} - A\Delta t\Delta_{h,(4)}(\phi^{k+1} - \phi^k). \tag{3.10}$$

In comparison with the standard BDF algorithm, the concave diffusion term is updated explicitly, for the sake of unique solvability. In addition, a second order Douglas-Dupont-type regularization term is added in the chemical potential. Similar ideas could be found in [67], with the finite element approximation in space, and [27], in which the epitaxial thin film growth model is analyzed.

**Remark 3.3.** *For the rectangular domains considered in this article, other than the fourth order finite difference algorithm, the implementation of higher order finite element method is also feasible, while with more involved details. The use of $C^0$-cubic elements for $\phi$ and the chemical potential would be relatively straightforward, and the fourth order numerical accuracy in space could be carefully obtained, with at least $H^4$ regularity assumption for $\phi$, $\phi_t$ and $\phi_{tt}$. On the other hand, most computational challenges in this approach are focused on the numerical evaluation of the integrals for the nonlinear terms, since one would have to develop a quadrature rule to handle the nonlinear integrals. In addition, one could also do various cross-product finite element spaces with $C^1$-cubic elements or, again, just $C^0$-cubic elements.*

We denote $\Phi$ as the exact solution for (1.2), and the initial value is taken as $\phi_{i,j}^0 = \Phi(x_i, y_j, t = 0)$. In addition, it is noticed that (3.9)-(3.10) is a two-step numerical method, so that a "ghost" point extrapolation for $\phi^{-1}$ is needed. To preserve the second order accuracy in time, we apply the following approximation:

$$\phi^{-1} = \phi^0 - \Delta t\Delta_{h,(4)}\mu_h^0, \quad \text{with } \mu_h^0 := (\phi^0)^3 - \phi^0 - \varepsilon^2\Delta_{h,(4)}\phi^0. \tag{3.11}$$

A careful Taylor expansion indicates an $O(\Delta t^2 + h^4)$ accuracy for such an approximation:

$$\|\phi^{-1} - \Phi^{-1}\|_2 \le C(\Delta t^2 + h^4). \tag{3.12}$$

**Theorem 3.4.** *Given $\phi^k, \phi^{k-1} \in \mathcal{V}_{\rm per}$, with $\overline{\phi^k} = \overline{\phi^{k-1}}$, there exists a unique solution $\phi^{k+1} \in \mathcal{V}_{\rm per}$ for the numerical scheme* (3.9)-(3.10)*. And also, this scheme is mass conservative, i.e., $\overline{\phi^k} \equiv \overline{\phi^0} := \beta_0$, for any $k \ge 0$.*

**Theorem 3.5.** *For $k \ge 1$, we introduce*

$$\mathcal{E}_h(\phi^{k+1}, \phi^k) := E_h(\phi^{k+1}) + \frac{1}{4\Delta t}\|\phi^{k+1} - \phi^k\|_{-1,h}^2 + \frac{1}{2}\|\phi^{k+1} - \phi^k\|_2^2. \tag{3.13}$$

*For $A \ge \frac{1}{16}$, a modified energy-decay property is available for the numerical scheme* (3.9)-(3.10)*:*

$$\mathcal{E}_h(\phi^{k+1}, \phi^k) \le \mathcal{E}_h(\phi^k, \phi^{k-1}). \tag{3.14}$$

**Remark 3.6.** *The energy stability for a gradient flow has always played an essential role in the accuracy of long time numerical simulation. Originated from the pioneering references [22, 24], the related works could also be found for many related physical models, such as the phase field crystal (PFC) equation and the modified version [3, 4, 41, 62, 66]; epitaxial thin film growth models [8, 11,*

*57, 61]; non-local gradient model [34, 35, 36]; the Cahn-Hilliard model coupled with fluid flow [10, 14, 29, 54, 64]; etc. Meanwhile, most of these works are associated with either the second order centered difference or finite element spatial approximations; this article is the first work to justify the energy stability for a fourth order finite difference scheme, combined with a second order temporal accuracy.*

**Remark 3.7.** *The pioneering numerical algorithm of second order accurate (in time), energy stable scheme for the Cahn-Hilliard equation could be found in the work of Du & Nicolaides [17], with many subsequent follow-ups. Such a numerical approach is based on the standard Crank-Nicolson approximation, with a slight modification in the nonlinear approximation. One challenge associated with this numerical scheme is the theoretical justification of the unique solvability, which comes from the Crank-Nicolson approximation to the concave diffusion term. In more details, the unique solvability for this numerical scheme is ensured under a time step constraint: $\Delta t \le C h^2$, because of the implicit treatment of the concave term. A few more recent works [13, 37] have used a second order explicit extrapolation formula for the concave term, so that the unique solvability and energy stability could be both satisfied. Another computational challenge in the numerical implementation of the scheme reported in [17] comes from a special quadrature rule needed in the nonlinear integration, which is associated with its Galerkin feature. In comparison, the finite difference implementation of the nonlinear terms in* (3.9)-(3.10) *is more straightforward, due to its collocation feature.*

As a direct consequence of the energy stability, a uniform in time $H_h^1$ bound for the numerical solution is given as follows.

**Corollary 3.8.** *Suppose that the initial data are sufficiently regular so that*

$$E_h(\phi^0) + \frac{\Delta t}{4}\|\nabla_{h,(4)}\mu_h^0\|_2^2 + \frac{\Delta t^2}{2}\|\Delta_{h,(4)}\mu_h^0\|_2^2 \le \tilde{C}_0,$$

*for some $\tilde{C}_0$ that is independent of $h$, and $A \ge \frac{1}{16}$. Then we have the following uniform (in time) $H_h^1$ bound for the numerical solution:*

$$\|\phi^m\|_{H_h^1} \le \tilde{C}_1, \quad \forall m \ge 1, \tag{3.15}$$

*in which $\tilde{C}_1$ only depends on $\Omega$, $\varepsilon$ and $\tilde{C}_0$, independent on $h$, $\Delta t$ and final time.*

With an initial data with sufficient regularity, we could assume that the exact solution has regularity of class $\mathcal{R}$:

$$\Phi \in \mathcal{R} := H^3(0,T;C^0) \cap H^2(0,T;H^4) \cap L^\infty(0,T;H^8). \tag{3.16}$$

**Theorem 3.9.** *Given initial data $\Phi_0 \in H^8_{\rm per}(\Omega)$, suppose the exact solution for Cahn-Hilliard equation* (1.2) *is of regularity class $\mathcal{R}$. Then, provided $\Delta t$ and $h$ are sufficiently small, for all positive integers $n$, such that $n\Delta t \le T$, we have*

$$\|\Phi^n - \phi^n\|_2 + (\varepsilon^2 \Delta t \sum_{m=1}^{n} \|\Delta_h(\Phi^m - \phi^m)\|_2^2)^{1/2} \le C(\Delta t^2 + h^4), \tag{3.17}$$

*where $C > 0$ is independent of $\Delta t$ and $h$.*

# 4 The detailed proof

## 4.1 Proof of Theorem 3.4: unique solvability

*Proof.* We see that the scheme (3.9)-(3.10) can be rewritten as

$$\begin{aligned} \mathcal{N}_h[\phi] &= f, \qquad (4.1)\\ \text{with } \mathcal{N}_h[\phi] &:= -\Delta_{h,(4)}^{-1}\left(\frac{3}{2}\phi - 2\phi^k + \frac{1}{2}\phi^{k-1}\right) + \Delta t\phi^3 - \Delta t(A\Delta t + \varepsilon^2)\Delta_{h,(4)}\phi,\\ f &:= -2\Delta t\phi^k + \Delta t\phi^{k-1} + A\Delta t^2\Delta_{h,(4)}\phi^k. \end{aligned}$$

Meanwhile, the nonlinear equation (4.1) can be recast as a minimization problem for the following discrete energy functional:

$$F_h[\phi] := \frac{1}{3}\left\|\frac{3}{2}\phi - 2\phi^k + \frac{1}{2}\phi^{k-1}\right\|_{-1,h}^2 + \frac{\Delta t}{4}\|\phi\|_4^4 + \frac{\Delta t}{2}(A\Delta t + \varepsilon^2)\left\|\nabla_{h,(4)}\phi\right\|_2^2 - (f,\phi)_2, \qquad (4.2)$$

for any $\phi \in \mathcal{V}_{\text{per}}$. In turn, the strong convexity of $F_h$ (in terms of $\phi$), over the hyperplane of $\bar{\phi} = \beta_0$, implies a unique numerical solution for (3.9)-(3.10).

By taking a discrete summation of (3.9), and making use of the fact that $\overline{\Delta_{h,(4)}\mu_h^{k+1}} = 0$, as well as the mass conservation of the previous time steps: $\overline{\phi^k} = \overline{\phi^{k-1}} = \beta_0$, we are able to conclude that $\overline{\phi^{k+1}} = \beta_0$, for any $k \geq 0$. □

## 4.2 Proof of Theorem 3.5: energy stability

*Proof.* Since $\phi^{k+1} - \phi^k \in \mathring{\mathcal{V}}_{\text{per}}$, we take a discrete inner product with (3.9) by $(-\Delta_{h,(4)})^{-1}(\phi^{k+1} - \phi^k)$, with the following inequalities derived:

$$\begin{aligned} &\left(\frac{\frac{3}{2}\phi^{k+1} - 2\phi^k + \frac{1}{2}\phi^{k-1}}{2\Delta t}, (-\Delta_{h,(4)})^{-1}(\phi^{k+1} - \phi^k)\right)_2\\ =\ & \frac{1}{\Delta t}\left(\frac{3}{2}\left\|\phi^{k+1} - \phi^k\right\|_{-1,h}^2 - \frac{1}{2}(\phi^k - \phi^{k-1}, \phi^{k+1} - \phi^k)_{-1}\right)\\ \geq\ & \frac{1}{\Delta t}\left(\frac{5}{4}\left\|\phi^{k+1} - \phi^k\right\|_{-1,h}^2 - \frac{1}{4}\left\|\phi^k - \phi^{k-1}\right\|_{-1,h}^2\right), \qquad (4.3)\\ &\left(-\Delta_{h,(4)}((\phi^{k+1})^3), (-\Delta_{h,(4)})^{-1}(\phi^{k+1} - \phi^k)\right)_2\\ =\ & \left((\phi^{k+1})^3, \phi^{k+1} - \phi^k\right)_2 \geq \frac{1}{4}(\|\phi^{k+1}\|_4^4 - \|\phi^k\|_4^4), \qquad (4.4)\\ &\left(\Delta_{h,(4)}^2\phi^{k+1}, (-\Delta_{h,(4)})^{-1}(\phi^{k+1} - \phi^k)\right)_2 = \left(-\Delta_{h,(4)}\phi^{k+1}, \phi^{k+1} - \phi^k\right)_2\\ =\ & \frac{1}{2}\left(\|\nabla_{h,(4)}\phi^{k+1}\|^2 - \|\nabla_{h,(4)}\phi^k\|^2 + \|\nabla_{h,(4)}(\phi^{k+1} - \phi^k)\|^2\right), \qquad (4.5)\\ &\Delta t\left(\Delta_{h,(4)}^2(\phi^{k+1} - \phi^k), (-\Delta_{h,(4)})^{-1}(\phi^{k+1} - \phi^k)\right)_2 = \Delta t\|\nabla_{h,(4)}(\phi^{k+1} - \phi^k)\|^2, \qquad (4.6)\\ &\left(\Delta_{h,(4)}(2\phi^k - \phi^{k-1}), (-\Delta_{h,(4)})^{-1}(\phi^{k+1} - \phi^k)\right)_2 = -\left(2\phi^k - \phi^{k-1}, \phi^{k+1} - \phi^k\right)_2\\ \geq\ & -\frac{1}{2}\left(\|\phi^{k+1}\|_2^2 - \|\phi^k\|_2^2\right) - \frac{1}{2}\|\phi^k - \phi^{k-1}\|_2^2. \qquad (4.7) \end{aligned}$$

Meanwhile, an application of Cauchy inequality indicates the following estimate:

$$\begin{aligned} & \frac{1}{\Delta t}\left\|\phi^{k+1}-\phi^{k}\right\|_{-1,h}^{2}+A\Delta t\|\nabla_{h,(4)}(\phi^{k+1}-\phi^{k})\|_{2}^{2} \\ \geq\ & 2A^{1/2}\left\|\phi^{n+1}-\phi^{n}\right\|_{-1,h}\cdot\|\nabla_{h,(4)}(\phi^{n+1}-\phi^{n})\|_{2}\geq 2A^{1/2}\|\phi^{n+1}-\phi^{n}\|_{2}^{2}, \end{aligned} \tag{4.8}$$

in which (3.7) (in Lemma 3.2) has been used in the second step. In turn, a combination of (4.3)-(4.7) and (4.8) yields

$$\begin{aligned} & E_h(\phi^{k+1})-E_h(\phi^{k})+\frac{1}{4\Delta t}\left(\|\phi^{k+1}-\phi^{k}\|_{-1,h}^{2}-\|\phi^{k}-\phi^{k-1}\|_{-1,h}^{2}\right) \\ & +\frac{1}{2}\left(\|\phi^{n+1}-\phi^{n}\|_{2}^{2}-\|\phi^{n}-\phi^{n-1}\|_{2}^{2}\right)\leq(-2A^{1/2}+\frac{1}{2})\|\phi^{n+1}-\phi^{n}\|_{2}^{2}\leq 0, \quad \text{if } A\geq\tfrac{1}{16}. \end{aligned} \tag{4.9}$$

Then we arrive at (3.14), provided that $A\geq\frac{1}{16}$. This completes the proof of Theorem 3.5. □

### 4.3 Proof of Corollary 3.8: uniform in time $H_h^1$ bound

*Proof.* As a result of (3.14), the following energy bound is available:

$$\begin{aligned} E_h(\phi^{m}) &\leq \mathcal{E}_h(\phi^{m},\phi^{m-1})\leq\mathcal{E}_h(\phi^{0},\phi^{-1})=E_h(\phi^{0})+\frac{1}{4\Delta t}\|\phi^{0}-\phi^{-1}\|_{-1,h}^{2}+\frac{1}{2}\|\phi^{0}-\phi^{-1}\|_{2}^{2} \\ &= E_h(\phi^{0})+\frac{\Delta t}{4}\|\nabla_{h,(4)}\mu_h^{0}\|_{2}^{2}+\frac{\Delta t^{2}}{2}\|\Delta_{h,(4)}\mu_h^{0}\|_{2}^{2}\leq\tilde{C}_0, \quad \forall m\geq 1. \end{aligned} \tag{4.10}$$

On the other hand, the point-wise quadratic inequality, $\frac{1}{8}\phi^4-\frac{1}{2}\phi^2\geq-\frac{1}{2}$, implies that

$$\frac{1}{8}\|\phi^{m}\|_{4}^{4}-\frac{1}{2}\|\phi^{m}\|_{2}^{2}\geq-\frac{1}{2}|\Omega|. \tag{4.11}$$

Its substitution into (4.10) yields

$$\frac{1}{2}\|\phi^{m}\|_{2}^{2}+\frac{\varepsilon^{2}}{2}\|\nabla_{h,(4)}\phi^{m}\|_{2}^{2}\leq\tilde{C}_0+\frac{3}{4}|\Omega|, \text{ so that } \|\phi^{m}\|_{2}^{2}+\|\nabla_{h,(4)}\phi^{m}\|_{2}^{2}\leq 2\varepsilon^{-2}(\tilde{C}_0+\frac{3}{4}|\Omega|). \tag{4.12}$$

In turn, we arrive at

$$\begin{aligned} & \|\phi^{m}\|_{H_h^1}^{2}\leq\|\phi^{m}\|_{2}^{2}+\|\nabla_h\phi^{m}\|_{2}^{2}\leq\|\phi^{m}\|_{2}^{2}+\|\nabla_{h,(4)}\phi^{m}\|_{2}^{2}\leq 2\varepsilon^{-2}(\tilde{C}_0+\frac{3}{4}|\Omega|), \\ & \text{so that} \quad \|\phi^{m}\|_{H_h^1}\leq\varepsilon^{-1}\Big(2(\tilde{C}_0+\frac{3}{4}|\Omega|)\Big)^{1/2}:=\tilde{C}_1, \quad \forall m\geq 1, \end{aligned} \tag{4.13}$$

in which the second step comes from an obvious fact that $\|\nabla_h\phi^{m}\|_{2}\leq\|\nabla_{h,(4)}\phi^{m}\|_{2}$. This completes the proof of Corollary 3.8. □

**Remark 4.1.** *As a combination of the uniform in time $H_h^1$ bound* (3.15) *and the discrete Sobolev embedding inequality* (3.6)*, we arrive at a uniform in time $\ell^6$ estimate for the numerical solution:*

$$\|\phi^{m}\|_{6}\leq C\tilde{C}_1, \quad \forall m\geq 1. \tag{4.14}$$

*This estimate will be useful in the convergence analysis presented below.*

### 4.4 Proof of Theorem 3.9: the $\ell^2(0,T;\ell^2)\cap\ell^2(0,T;H_h^2)$ convergence analysis

Before the $\ell^2(0,T;\ell^2)\cap\ell^2(0,T;H_h^2)$ convergence analysis, we recall a modified version of discrete Gronwall inequality, excerpted from [15]; this result will be used in the convergence estimate, due to the 2nd order BDF stencil.

**Lemma 4.2.** *[15] Fix $T>0$. Let $M$ be a positive integer, with $\Delta t\le\frac{T}{M}$. Suppose $\{a_m\}_{m=0}^M$, $\{b_m\}_{m=0}^M$ and $\{c_m\}_{m=0}^{M-1}$ are non-negative sequences such that $\Delta t\sum_{m=0}^{M-1}c_m\le D_1$, with $D_1$ independent of $\Delta t$ and $M$. Suppose that, for all $\Delta t>0$ and for some constant $0<\alpha<1$,*

$$a_\ell+\Delta t\sum_{m=0}^{\ell}b_m\le D_2+\Delta t\sum_{m=0}^{\ell-1}c_m\sum_{j=0}^{m}\alpha^{m-j}a_j,\quad\forall\,1\le\ell\le M,\tag{4.15}$$

*where $D_2>0$ is a constant independent of $\Delta t$ and $M$. Then, for all $\Delta t>0$,*

$$a_\ell+\Delta t\sum_{m=0}^{\ell}b_m\le(D_2+a_0D_1)\exp\left(\frac{D_1}{1-\alpha}\right),\quad\forall\,1\le\ell\le M.\tag{4.16}$$

*Proof.* For $\Phi\in\mathcal{R}$, a careful consistency analysis indicates the following truncation error estimate:

$$\begin{aligned}\frac{\frac{3}{2}\Phi^{k+1}-2\Phi^k+\frac{1}{2}\Phi^{k-1}}{\Delta t}&=\Delta_{h,(4)}\Big((\Phi^{k+1})^3-2\Phi^k+\Phi^{k-1}-\varepsilon^2\Delta_{h,(4)}\Phi^{k+1}\\&\quad-A\Delta t\Delta_{h,(4)}(\Phi^{k+1}-\Phi^k)\Big)+\tau^{k+1},\end{aligned}\tag{4.17}$$

with $\|\tau^{k+1}\|_2\le C(\Delta t^2+h^4)$. The derivation of (4.17) is accomplished with the help of Proposition 2.4 and other related estimates; the details are left to interested readers.

The numerical error function is defined at a point-wise level:

$$\tilde\phi^k:=\Phi^k-\phi^k,\quad\forall m\ge0,\tag{4.18}$$

In turn, subtracting the numerical scheme (3.9)-(3.10) from (4.17) gives

$$\begin{aligned}\frac{\frac{3}{2}\tilde\phi^{k+1}-2\tilde\phi^k+\frac{1}{2}\tilde\phi^{k-1}}{\Delta t}&=\Delta_{h,(4)}\Big(\mathcal{NL}(\Phi^{k+1},\phi^{k+1})-2\tilde\phi^k+\tilde\phi^{k-1}-\varepsilon^2\Delta_{h,(4)}\tilde\phi^{k+1}\\&\quad-A\Delta t\Delta_{h,(4)}(\tilde\phi^{k+1}-\tilde\phi^k)\Big)+\tau^{k+1},\end{aligned}\tag{4.19}$$

$$\text{with}\quad\mathcal{NL}(\Phi^{k+1},\phi^{k+1})=((\Phi^{k+1})^2+\Phi^{k+1}\phi^{k+1}+(\phi^{k+1})^2)\tilde\phi^{k+1}.\tag{4.20}$$

Taking a discrete inner product with (4.19)-(4.20) by $\tilde\phi^{k+1}$, with a repeated application of summation by parts, we get

$$\begin{aligned}&\Big(\frac{3}{2}\tilde\phi^{k+1}-2\tilde\phi^k+\frac{1}{2}\tilde\phi^{k-1},\tilde\phi^{k+1}\Big)_2+\varepsilon^2\Delta t\|\Delta_{h,(4)}\tilde\phi^{k+1}\|_2^2+A\Delta t^2\Big(\Delta_{h,(4)}(\tilde\phi^{k+1}-\tilde\phi^k),\Delta_{h,(4)}\tilde\phi^{k+1}\Big)_2\\=\;&\Delta t\Big(\mathcal{NL}(\Phi^{k+1},\phi^{k+1}),\Delta_{h,(4)}\tilde\phi^{k+1}\Big)_2+\Delta t(\tilde\phi^{k+1},\tau^{k+1})_2.\end{aligned}\tag{4.21}$$

The time marching term could be analyzed as follows:

$$\begin{aligned}&\Big(\frac{3}{2}\tilde\phi^{k+1}-2\tilde\phi^k+\frac{1}{2}\tilde\phi^{k-1},\tilde\phi^{k+1}\Big)_2=\frac{3}{2}\Big(\tilde\phi^{k+1}-\tilde\phi^k,\tilde\phi^{k+1}\Big)_2-\frac{1}{2}\Big(\tilde\phi^k-\tilde\phi^{k-1},\tilde\phi^{k+1}\Big)_2\\\ge\;&\Big(\frac{3}{4}\|\tilde\phi^{k+1}\|_2^2-\frac{1}{4}\|\tilde\phi^k\|_2^2\Big)-\Big(\frac{3}{4}\|\tilde\phi^k\|_2^2-\frac{1}{4}\|\tilde\phi^{k-1}\|_2^2\Big)+\frac{1}{2}\Big(\|\tilde\phi^{k+1}-\tilde\phi^k\|_2^2-\|\tilde\phi^k-\tilde\phi^{k-1}\|_2^2\Big)\end{aligned}\tag{4.22}$$

The third term on the left hand side of (4.21) could be handled as follows:

$$\Big(\Delta_{h,(4)}(\tilde{\phi}^{k+1}-\tilde{\phi}^{k}),\Delta_{h,(4)}\tilde{\phi}^{k+1}\Big)_2\geq\frac{1}{2}(\|\Delta_{h,(4)}\tilde{\phi}^{k+1}\|_2^2-\|\Delta_{h,(4)}\tilde{\phi}^{k}\|_2^2). \tag{4.23}$$

The term associated with the local truncation error could be bounded with the help of Cauchy inequality:

$$(\tilde{\phi}^{k+1},\tau^{k+1})_2\leq\|\tilde{\phi}^{k+1}\|_2\cdot\|\tau^{k+1}\|_2\leq\frac{1}{2}(\|\tilde{\phi}^{k+1}\|_2^2+\|\tau^{k+1}\|_2^2). \tag{4.24}$$

For the nonlinear error term, we begin with an application of discrete Hölder inequality:

$$\begin{aligned}\|\mathcal{NL}(\Phi^{k+1},\phi^{k+1})\|_2 &\leq \|(\Phi^{k+1})^2+\Phi^{k+1}\phi^{k+1}+(\phi^{k+1})^2\|_3\cdot\|\tilde{\phi}^{k+1}\|_6\\ &\leq C(\|\Phi^{k+1}\|_6^2+\|\phi^{k+1}\|_6^2)\|\tilde{\phi}^{k+1}\|_6\leq C((C^*)^2+\tilde{C}_1^2)\|\tilde{\phi}^{k+1}\|_6,\end{aligned} \tag{4.25}$$

in which the estimates $\|\Phi^{k+1}\|_6\leq C^*$, and $\|\phi^{k+1}\|_6\leq C\tilde{C}_1$ (which comes from the uniform in time estimate (4.14) for the numerical solution, as given by Remark 4.1), have been used. On the other hand, we make use of the discrete Sobolev embedding inequality (3.6) again, and obtain

$$\begin{aligned}\|\tilde{\phi}^{k+1}\|_6 &\leq C(\|\tilde{\phi}^{k+1}\|_2+\|\nabla_h\tilde{\phi}^{k+1}\|_2)\leq C(\|\tilde{\phi}^{k+1}\|_2+\|\nabla_{h,(4)}\tilde{\phi}^{k+1}\|_2)\\ &\leq C(\|\tilde{\phi}^{k+1}\|_2+\|\tilde{\phi}^{k+1}\|_2^{1/2}\cdot\|\Delta_{h,(4)}\tilde{\phi}^{k+1}\|_2^{1/2}),\end{aligned} \tag{4.26}$$

in which the second step comes from the fact that $\|\nabla_h\tilde{\phi}^{k+1}\|_2\leq\|\nabla_{h,(4)}\tilde{\phi}^{k+1}\|_2$, while the last step is based on the following estimate:

$$\|\nabla_{h,(4)}\tilde{\phi}^{k+1}\|_2^2=(\tilde{\phi}^{k+1},-\Delta_{h,(4)}\tilde{\phi}^{k+1})_2\leq\|\tilde{\phi}^{k+1}\|_2\cdot\|\Delta_{h,(4)}\tilde{\phi}^{k+1}\|_2. \tag{4.27}$$

Consequently, a substitution of (4.26) into (4.25) yields

$$\|\mathcal{NL}(\Phi^{k+1},\phi^{k+1})\|_2\leq\tilde{C}_2(\|\tilde{\phi}^{k+1}\|_2+\|\tilde{\phi}^{k+1}\|_2^{1/2}\cdot\|\Delta_{h,(4)}\tilde{\phi}^{k+1}\|_2^{1/2}), \tag{4.28}$$

with $\tilde{C}_2=C((C^*)^2+\tilde{C}_1^2)$. In turn, a bound for the nonlinear error inner product term could be derived:

$$\begin{aligned}\Big(\mathcal{NL}(\Phi^{k+1},\phi^{k+1}),\Delta_{h,(4)}\tilde{\phi}^{k+1}\Big)_2 &\leq \|\mathcal{NL}(\Phi^{k+1},\phi^{k+1})\|_2\cdot\|\Delta_{h,(4)}\tilde{\phi}^{k+1}\|_2\\ &\leq \tilde{C}_2(\|\tilde{\phi}^{k+1}\|_2\cdot\|\Delta_{h,(4)}\tilde{\phi}^{k+1}\|_2+\|\tilde{\phi}^{k+1}\|_2^{1/2}\cdot\|\Delta_{h,(4)}\tilde{\phi}^{k+1}\|_2^{3/2})\\ &\leq \tilde{C}_{3,\varepsilon}\|\tilde{\phi}^{k+1}\|_2^2+\frac{\varepsilon^2}{2}\|\Delta_{h,(4)}\tilde{\phi}^{k+1}\|_2^2,\end{aligned} \tag{4.29}$$

with the Young's inequality applied in the last step.

Subsequently, a substitution of (4.22)-(4.24) and (4.29) into (4.21) yields

$$\mathcal{G}^{k+1}-\mathcal{G}^{k}+\frac{\varepsilon^2}{2}\Delta t\|\Delta_{h,(4)}\tilde{\phi}^{k+1}\|_2^2\leq(\tilde{C}_{3,\varepsilon}+\frac{1}{2})\Delta t\|\tilde{\phi}^{k+1}\|_2^2+\Delta t\|\tau^{k+1}\|_2^2, \tag{4.30}$$

$$\text{with}\quad \mathcal{G}^{k+1}:=\frac{3}{4}\|\tilde{\phi}^{k+1}\|_2^2-\frac{1}{4}\|\tilde{\phi}^{k}\|_2^2+\frac{1}{2}\|\tilde{\phi}^{k+1}-\tilde{\phi}^{k}\|_2^2+\frac{A}{2}\Delta t^2\|\Delta_{h,(4)}\tilde{\phi}^{k+1}\|_2^2. \tag{4.31}$$

Meanwhile, for the term $\|\tilde{\phi}^{k+1}\|_2^2$, the following inductive estimate is available:

$$\begin{aligned}\|\tilde{\phi}^{k+1}\|_2^2 &\leq \frac{4}{3}\mathcal{G}^{k+1}+\frac{1}{3}\|\tilde{\phi}^{k}\|_2^2\leq\frac{4}{3}\mathcal{G}^{k+1}+\frac{4}{9}\mathcal{G}^{k}+\frac{1}{9}\|\tilde{\phi}^{k-1}\|_2^2\leq\ldots\\ &\leq \frac{4}{3}\sum_{i=0}^{k+1}(\frac{1}{3})^i\mathcal{G}^{k+1-i}.\end{aligned} \tag{4.32}$$

This in turn leads to the following inequality

$$\mathcal{G}^{k+1}-\mathcal{G}^k+\frac{\varepsilon^2}{2}\Delta t\|\Delta_{h,(4)}\tilde{\phi}^{k+1}\|_2^2\le\frac{4}{3}(\tilde{C}_{3,\varepsilon}+\frac{1}{2})\Delta t\sum_{i=0}^{k+1}(\frac{1}{3})^i\mathcal{G}^{k+1-i}+\Delta t\|\tau^{k+1}\|_2^2. \tag{4.33}$$

Therefore, with an application of Lemma 4.2, and making use of the fact that $\|\tau^{k+1}\|_2\le C(\Delta t^2+h^4)$, we conclude that

$$\mathcal{G}^{k+1}+\varepsilon^2\Delta t\sum_{i=1}^{k+1}\|\Delta_{h,(4)}\tilde{\phi}^i\|_2^2\le\hat{C}(\Delta t^4+h^8), \tag{4.34}$$

with $\hat{C}$ independent on $\Delta t$ and $h$. Furthermore, with an application of (4.32), we arrive at the desired convergence estimate:

$$\|\tilde{\phi}^{k+1}\|_2+\Big(\varepsilon^2\Delta t\sum_{i=1}^{k+1}\|\Delta_h\tilde{\phi}^i\|_2^2\Big)^{1/2}\le C\hat{C}^{1/2}(\Delta t^2+h^4), \tag{4.35}$$

This completes the proof of Theorem 3.9. □

**Remark 4.3.** *The phase field models, such as Allen-Cahn and Cahn-Hillird equations, have a broader impact on many scientific disciplines. A detailed study of these nonlinear gradient flows is vital for understanding phase transformations of materials at the atomic and nanometer scales, the complex processes in biological growth and development, etc. A coupling of phase field model and fluid motion, such as the Cahn-Hilliard-Navier-Stokes equation [51], turns out be be even more interesting, since its ability to describe multi-phase flows and its application in tumor growth evolution. Many techniques in the numerical analysis for the phase field models could be applied to these coupled systems, with more careful treatments for the nonlinear coupled convection terms. See the related error estimates in recent years [9, 10, 14, 15, 54]; many more such works are also expected in the future works.*

**Remark 4.4.** *Other than the finite difference analysis presented in this article, there have been extensive works on the finite element analysis for the Cahn-Hilliard equation, such as [2, 18, 19, 21, 23], etc. In fact, many ideas in the stability and convergence estimates for these two different numerical approaches have followed similar mathematical principles; while the technical details have to be presented in different forms.*

## 5 Numerical results

The numerical implementation of the proposed fourth order finite difference scheme (3.9)-(3.10) requires a nonlinear solver. Meanwhile, since the nonlinear term corresponds to a convex functional, as indicated by (4.2), some ideas associated with convex optimization could be efficiently applied. We use the precondition steepest descent (PSD) iteration to implement this numerical algorithm; such an iteration has been proposed and analyzed for the regularized p-Laplacian problem in recent works [26, 27], and its extension to Cahn-Hilliard-type problem is straightforward.

### 5.1 Precondition steepest descent (PSD) solver

The main idea of the PSD solver is to use a linearized version of the nonlinear operator as a preconditioner, or in other words, as a metric for choosing the search direction. A linearized version of the nonlinear operator $\mathcal{L}_h : \mathring{\mathcal{V}}_{\rm per} \to \mathring{\mathcal{V}}_{\rm per}$, is defined as follows:

$$\mathcal{L}_h[\psi] := -\Delta_{h,(4)}^{-1}\psi + \Delta t\psi - \Delta t(\varepsilon^2 + A\Delta t)\Delta_{h,(4)}^2\psi. \tag{5.1}$$

Given the current iterate $\phi^{(n)} \in \mathcal{V}_{\rm per}$, we define the following *search direction* problem: find $d^{(n)} \in \mathring{\mathcal{V}}_{\rm per}$ such that

$$\mathcal{L}_h[d^{(n)}] = f - \mathcal{N}_h[\phi^{(n)}] := r^{(n)},$$

where $r^{(n)}$ is the nonlinear residual of the $n^{\rm th}$ iterate $\phi^{(n)}$. This equation can be solved efficiently using the Fast Fourier Transform (FFT).

In turn, the next iterate is given by

$$\phi^{(n+1)} = \phi^{(n)} + \overline{\alpha} d^{(n)}, \tag{5.2}$$

where $\overline{\alpha} \in \mathbb{R}$ is the unique solution to the steepest descent line minimization problem

$$\overline{\alpha} := \operatorname*{argmax}_{\alpha\in\mathbb{R}} F_h[\phi^{(n)} + \alpha d^{(n)}] = \operatorname*{argzero}_{\alpha\in\mathbb{R}} \delta F_h[\phi^{(n)} + \alpha d^{(n)}](d^{(n)}). \tag{5.3}$$

The geometric convergence analysis of the PSD solver has been established in [26], for egularized p-Laplacian problem. For the Cahn-Hilliard-type problem (3.9)-(3.10), the corresponding nonlinearity is weaker than that of the p-Laplacian problem, and the geometric convergence rate: $\phi^{(n)} \to \phi^{k+1}$, (where $\phi^{k+1}$ is the exact numerical solution to (3.9)-(3.10)), as $n \to \infty$, is expected to be derived in a similar way; the details are left to interested readers.

### 5.2 Convergence test for the numerical scheme

In this subsection we perform some numerical experiments to support the theoretical results, using a uniform Cartesian grid and set periodic boundary conditions. In particular, it is observed that the search direction and Poisson-like equations can also be efficiently solved efficiently by using the Fourier pseudo-spectral method (see the related discussions in [5, 12, 33, 40]) and Fast Fourier Transform (FFT).

To test the convergence rate, we choose the data such that the exact solution of (1.2) on the square domain $\Omega = (0, 3.2) \times (0, 3.2)$:

$$\phi_e(x, y, t) = \frac{1}{2\pi} \sin\big(2\pi x/3.2\big) \cos\big(2\pi y/3.2\big) \cos(t). \tag{5.4}$$

We take a quadratic refinement path for scheme (3.9)-(3.10) , i.e. $\Delta t = Ch^2$. The final time is taken as $T = 0.32$, and we expect the global error to be $\mathcal{O}(h^4)$ under the $\|\cdot\|_\infty$ and $\|\cdot\|_2$ norm, as $h, \Delta t \to 0$. The other parameter are given by $L_x = L_y = 3.2$, $\varepsilon = 0.1$.

To investigate the accuracy in space, we fix $\Delta t = 10^{-4}$ so that the temporal numerical error is negligible, and we compute solutions with grid sizes $N = 32$ to$N = 128$ in increments of 16, and we solve up to time $T = 0.32$. The numerical errors are displayed in Table 1; the fourth order spatial accuracy is apparently observed for the phase variable.

To explore the temporal accuracy, we fix the spatial resolution as $N = 256$ so that the numerical error is dominated by the temporal ones. We compute solutions with a sequence of time step sizes, $\Delta t = \frac{T}{N_k}$, with $N_k = 100$ to $N_k = 500$ in increments of 100, and the same final time $T = 0.32$. Table 2 shows the discrete $\ell^2$ and $\ell^\infty$ norms of the errors between the numerical and exact solutions. A clear second-order accuracy is observed for the phase variable.

Table 1: Discrete $\ell^2$ and $\ell^\infty$ error norms and the convergence rates for the computed solution with scheme (3.9)-(3.10). The time step size is fixed as $\Delta t = 10^{-4}$.

| $h$ | $\|\phi - \mathcal{I}_h\phi_e\|_\infty$ | Rate | $\|\phi - \mathcal{I}_h\phi_e\|_2$ | Rate |
|---|---|---|---|---|
| $\frac{3.2}{32}$ | $2.8431 \times 10^{-6}$ | - | $4.5964 \times 10^{-6}$ | - |
| $\frac{3.2}{48}$ | $5.6591 \times 10^{-7}$ | 3.98 | $9.1001 \times 10^{-7}$ | 3.99 |
| $\frac{3.2}{64}$ | $1.7970 \times 10^{-7}$ | 3.99 | $2.8843 \times 10^{-7}$ | 3.99 |
| $\frac{3.2}{80}$ | $7.3859 \times 10^{-8}$ | 3.98 | $1.1845 \times 10^{-7}$ | 3.99 |
| $\frac{3.2}{96}$ | $3.5787 \times 10^{-8}$ | 3.97 | $5.7364 \times 10^{-8}$ | 3.98 |
| $\frac{3.2}{112}$ | $1.9454 \times 10^{-8}$ | 3.96 | $3.1174 \times 10^{-8}$ | 3.96 |
| $\frac{3.2}{128}$ | $1.1523 \times 10^{-8}$ | 3.94 | $1.8461 \times 10^{-8}$ | 3.94 |

Table 2: Discrete $\ell^2$ and $\ell^\infty$ error norms and the convergence rates for the computed solution with scheme (3.9)-(3.10). The spatial resolution isfixed as $N = 256$.

| $\Delta t$ | $\|\phi - \mathcal{I}_h\phi_e\|_\infty$ | Rate | $\|\phi - \mathcal{I}_h\phi_e\|_2$ | Rate |
|---|---|---|---|---|
| $\frac{0.32}{100}$ | $2.8918 \times 10^{-7}$ | - | $4.6310 \times 10^{-7}$ | - |
| $\frac{0.32}{200}$ | $7.2833 \times 10^{-8}$ | 1.99 | $1.1664 \times 10^{-7}$ | 1.99 |
| $\frac{0.32}{300}$ | $3.2762 \times 10^{-8}$ | 1.97 | $5.2466 \times 10^{-8}$ | 1.97 |
| $\frac{0.32}{400}$ | $1.8737 \times 10^{-8}$ | 1.95 | $3.0006 \times 10^{-8}$ | 1.95 |
| $\frac{0.32}{500}$ | $1.2241 \times 10^{-8}$ | 1.92 | $1.9604 \times 10^{-8}$ | 1.92 |

### 5.3 Numerical simulation of spinodal decomposition and energy dissipation

We simulate the spinodal decomposition of a mixed binary fluid and present the energy dissipation in this subsection. The parameters are given by $L_x = L_y = 12.8$, $\varepsilon = 0.03$, $h = 12.8/512$,. The initial data for this simulation is taken as a random field values $\phi^0_{i,j} = \bar{\phi} + 0.1 \cdot (2r_{i,j} - 1)$, with an average composition $\bar{\phi} = 0$ and $r_{i,j} \in [0, 1]$. For the temporal step size $\Delta t$, we use increasing values of $\Delta t$ in the time evolution: $\Delta t = 0.01$ on the time interval $[0, 2000]$ and $\Delta t = 0.04$ on the time interval $[2000, 6000]$. Whenever a new time step size is applied, we initiate the two-step numerical scheme by taking $\phi^{-1} = \phi^0$, with the initial data $\phi^0$ given by the final time output of the last time period. The snapshots of spinodal decomposition for the proposed numerical scheme, with second order accuracy in time and fourth order accuracy in space, can be found in Figure 1. The corresponding energy decay plot is displayed in Figure 2.

The log-log plots of energy evolution and the corresponding linear regression in Figure 2 shows that the energy indeed decays like $t^{-1/3}$ for the proposed scheme, which verifies the one-third power law. The detailed scaling "exponent" is obtained using least squares fits of the computed data up to time $t = 400$. A clear observation of the $a_e t^{-b_e}$ scaling law can be made, with $a_e = 2.3670$, $b_e = 0.3332$. In other words, an almost perfect $t^{-1/3}$ energy dissipation law is confirmed by our numerical simulation.

The linear regressions is only taken up to $t = 6000$, since the saturation time would be of the order of $\varepsilon^{-2}$.

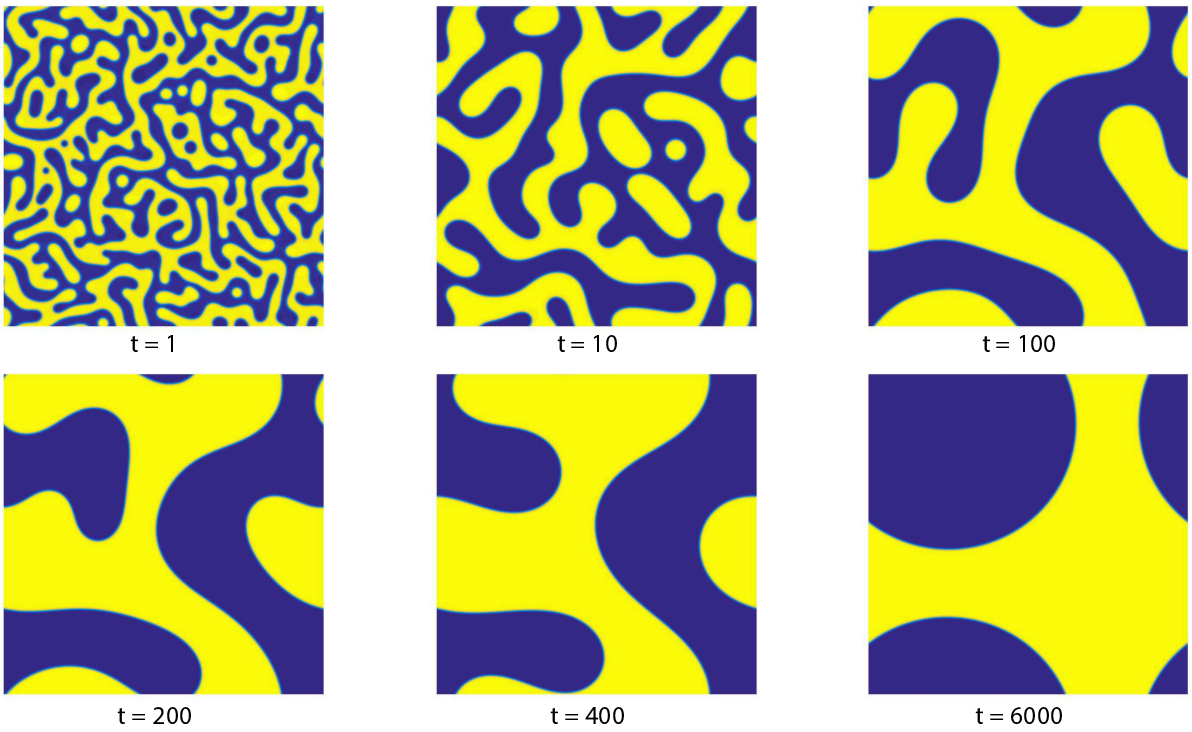


Figure 1: (Color online). Snapshots of spinodal decomposition of Cahn-Hilliard equation for a mixed binary fluid with scheme (3.9)-(3.10) in $\Omega = (0, 12.8) \times (0, 12.8)$ at a sequence of time instants: 1, 10, 100, 200, 400 and 2000. The surface diffusion parameter is taken to be $\varepsilon = 0.03$ and the time step size is $\Delta t = 0.01$.

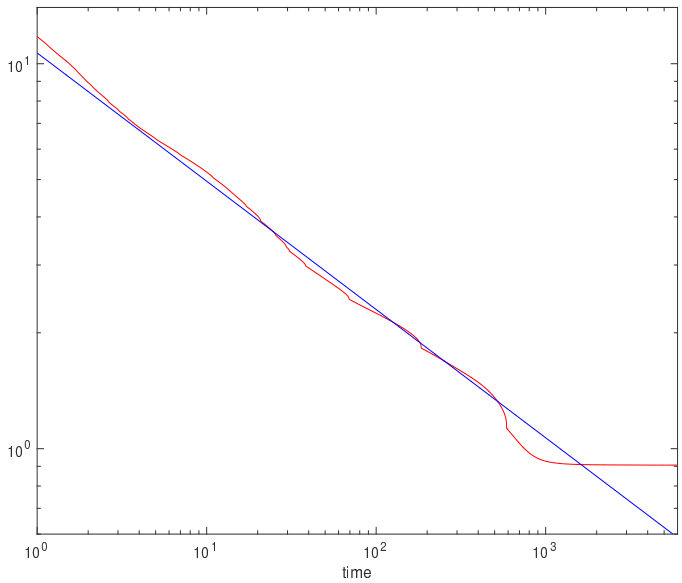


Figure 2: The evolutions of discrete energy. The parameters are given in the text and in the caption of Figure 1. The energy decays like $t^{-1/3}$, which verifies the one-third power law. More precisely, the linear fit has the form $a_e t^{-b_e}$ with $a_e = 2.3670, b_e = 0.3332$.

# 6 Concluding remarks

In this article, we propose and analyze an energy stable fourth order finite difference scheme for the Cahn-Hilliard equation, with second order temporal accuracy. As a preliminary truncation error estimate for the long stencil difference operator, over a uniform numerical grid with a periodic boundary condition, the discrete $\ell^2$ estimate only requires an $H^m$ regularity for the test function, which in turn results in a reduced regularity requirement. In the temporal approximation, we apply a modified BDF algorithm, combined with a second order extrapolation formula applied to the concave term. And also, a second order artificial Douglas-Dupont regularization is included in the numerical scheme, to ensure the energy stability at a discrete level. With such a careful construction, the unique solvability and energy stability are proved for the proposed numerical scheme, and a uniform in time $H_h^1$ bound for the numerical solution is established. As a result of this $H_h^1$ bound, we are able to derive an optimal rate convergence analysis for the proposed numerical scheme, in the $\ell^\infty(0,T;\ell^2)\cap\ell^2(0,T;H_h^2)$ norm. In addition, a few numerical experiments have confirmed these theoretical results, and the numerical simulations results of spinodal decomposition in a mixed binary fluid have indicated an energy dissipation law of $t^{-1/3}$.

# A Proof of Lemma 2.6

By substituting (2.38), we see that the first inequality of (2.46) is equivalent to

$$\left| -4\sin^2(k\pi h/L) - \frac{4}{3}\sin^4(k\pi h/L) + \frac{4k^2\pi^2h^2}{L^2} \right| \le C_1 h^6 \left(\frac{2k\pi}{L}\right)^6, \quad \forall\ 0 \le k \le N. \tag{A.1}$$

We denote $c_k = k\pi h/L$. Due to the fact that $h = \frac{L}{2N+1}$, we have

$$0 \le c_k \le \frac{\pi}{2}, \quad \forall\ 1 \le k \le N. \tag{A.2}$$

In turn, we need both the lower and upper bounds of $-4\sin^2 c_k - \frac{4}{3}\sin^4 c_k + 4c_k^2$ to establish the estimate (A.1). For the lower bound, the following inequality is observed:

$$h_1(t) := \sin^2 t + \frac{1}{3}\sin^4 t \le h_2(t) := t^2, \quad \forall\ t \ge 0. \tag{A.3}$$

The derivation of this inequality is based on the fact that

$$h_1(0) = h_2(0) = 0, \quad h_1'(0) = h_2'(0) = 0, \tag{A.4}$$

and a careful comparison between their second order derivatives:

$$h_1''(t) = 2\left(\cos^2 t + \sin^2 t\cos^2 t - \frac{5}{3}\sin^4 t\right) \le h_2''(t) = 2, \quad \forall\ t \ge 0. \tag{A.5}$$

As a result of (A.3), we obtain the following lower bound:

$$0 \le -4\sin^2 c_k - \frac{4}{3}\sin^4 c_k + 4c_k^2, \quad \forall\ 0 \le k \le N. \tag{A.6}$$

For the upper bound, we begin with a Taylor expansion for $\sin t$:

$$\sin t \ge t - \frac{t^3}{3!} = t - \frac{t^3}{6} \ge 0, \quad \forall\ 0 \le t \le \frac{\pi}{2}, \tag{A.7}$$

in which the second inequality comes from the range that $0 \le t \le \frac{\pi}{2}$. Subsequently, we set $c_k = k\pi h/L$ and arrive at

$$4\sin^2 c_k + \frac{4}{3}\sin^4 c_k \ge 4\left(c_k - \frac{c_k^3}{6}\right)^2 + \frac{4}{3}\left(c_k - \frac{c_k^3}{6}\right)^4 = 4c_k^2 - \frac{7}{9}c_k^6 + \frac{2}{9}c_k^8 - \frac{2}{81}c_k^{10} + \frac{1}{972}c_k^{12}, \quad \text{(A.8)}$$

for any $0 \le k \le N$. In turn, the following estimate is available:

$$-4\sin^2 c_k - \frac{4}{3}\sin^4 c_k + 4c_k^2 \le \frac{7}{9}c_k^6 - \frac{2}{9}c_k^8 + \frac{2}{81}c_k^{10} - \frac{1}{972}c_k^{12}, \quad \forall\ 0 \le k \le N. \quad \text{(A.9)}$$

Consequently, a combination of (A.6) and (A.9) results in

$$\left|-4\sin^2 c_k - \frac{4}{3}\sin^4 c_k + 4c_k^2\right| \le \frac{7}{9}c_k^6 - \frac{2}{9}c_k^8 + \frac{2}{81}c_k^{10} - \frac{1}{972}c_k^{12}, \quad \forall\ 0 \le k \le N. \quad \text{(A.10)}$$

On the other hand, by the definition $c_k = k\pi h/L$, the following estimates can be derived:

$$c_k^6 = h^6\left(k\pi/L\right)^6 \le \frac{1}{64}h^6\left(2k\pi/L\right)^6, \quad \forall\ 0 \le k \le N, \quad \text{(A.11)}$$

$$c_k^m = c_k^6 \cdot c_k^{m-6} \le \left(\frac{\pi}{2}\right)^{m-6} \cdot \frac{1}{64}h^6\left(2k\pi/L\right)^6, \quad \forall\ m \ge 6,\ 0 \le k \le N. \quad \text{(A.12)}$$

Finally, a combination of (A.10), (A.11) and (A.12) implies (A.1), with an appropriate choice of $C_1$. The proof of the first part of Lemma 2.6 is finished. The second inequality can be derived in the same manner.

# B Proof of Lemma 2.7

We see that the expansion for $\left\|\Delta^3 f\right\|_{L^2}$ in (2.34) can be decomposed in the following way:

$$\left\|\Delta^3 f\right\|_2^2 = \sum_{k,l=-N}^{N} I_{k,l}, \quad \text{with}$$

$$I_{k,l} = L^2 \sum_{k_1,l_1=-\infty}^{\infty}\left(\left(\frac{2(k+k_1N^*)\pi}{L}\right)^2 + \left(\frac{2(l+l_1N^*)\pi}{L}\right)^2\right)^6 \left|\hat{f}_{k+k_1N^*,l+l_1N^*}\right|^2. \quad \text{(B.1)}$$

In particular, we observe that

$$\left(\left(\frac{2(k+k_1N^*)\pi}{L}\right)^2 + \left(\frac{2(l+l_1N^*)\pi}{L}\right)^2\right)^6 \left|\hat{f}_{k+k_1N^*,l+l_1N^*}\right|^2 \le \frac{I_{k,l}}{L^2},$$

$$\text{i.e.} \quad \left|\hat{f}_{k+k_1N^*,l+l_1N^*}\right| \le \left(\left(\frac{2(k+k_1N^*)\pi}{L}\right)^2 + \left(\frac{2(l+l_1N^*)\pi}{L}\right)^2\right)^{-3}\sqrt{\frac{I_{k,l}}{L^3}}. \quad \text{(B.2)}$$

Meanwhile, the following fact is obvious

$$\left|\lambda_{kx,(4)} + \frac{4(k+k_1N^*)^2\pi^2}{L^2}\right| \le \frac{4(k+k_1N^*)^2\pi^2}{L^2}, \quad \text{since } \lambda_{kx,(4)} \le 0 \text{ and } |\lambda_{kx,(4)}| \le \tfrac{4k^2\pi^2}{L^2}. \quad \text{(B.3)}$$

Therefore, the following estimate is valid for a fixed $(k,l)$ and $(k_1,l_1)\neq(0,0)$:

$$\begin{aligned}
\left|\left(\lambda_{kx,(4)}+\frac{4(k+k_1N^*)^2\pi^2}{L^2}\right)\hat{f}_{k+k_1N^*,l+l_1N^*}\right| &\leq \frac{4(k+k_1N^*)^2\pi^2}{L^2}\left|\hat{f}_{k+k_1N^*,l+l_1N^*}\right| \\
&\leq \left(\left(\frac{2(k+k_1N^*)\pi}{L}\right)^2+\left(\frac{2(l+l_1N^*)\pi}{L}\right)^2\right)^{-2}\sqrt{\frac{I_{k,l}}{L^2}} \\
&\leq \left(\frac{4(N^*)^2\pi^2}{L^2}\left((|k_1|-\frac{1}{2})^2+(|l_1|-\frac{1}{2})^2\right)\right)^{-2}\sqrt{\frac{I_{k,l}}{L^2}} \\
&\leq \frac{1}{16}h^4\pi^{-4}\sqrt{\frac{I_{k,l}}{L^2}}\frac{1}{\left((|k_1|-\frac{1}{2})^2+(|l_1|-\frac{1}{2})^2\right)^2},
\end{aligned} \tag{B.4}$$

in which the grid size $h=\frac{L}{2N+1}$ was recalled. Also note that we used the following estimate in the third step

$$|k+k_1N^*|\geq\frac{(|k_1|-\frac{1}{2})N^*}{2},\quad |l+l_1N^*|\geq\frac{(|l_1|-\frac{1}{2})N^*}{2},\quad \text{for}\quad k_1\neq 0,\ l_1\neq 0, \tag{B.5}$$

due to the fact that $|k|,|l|\leq N^*/2$. Consequently, its substitution into (2.47) shows that

$$\begin{aligned}
&\left|\sum_{\substack{k_1,l_1=-\infty\\(k_1,l_1)\neq(0,0)}}^{\infty}\left(\lambda_{kx,(4)}+\frac{4(k+k_1N^*)^2\pi^2}{L^2}\right)\hat{f}_{k+k_1N^*,l+l_1N^*}\right| \\
&\quad\leq \sum_{\substack{k_1,l_1=-\infty\\(k_1,l_1)\neq(0,0)}}^{\infty}\left|\left(\lambda_{kx,(4)}+\frac{4(k+k_1N^*)^2\pi^2}{L^2}\right)\hat{f}_{k+k_1N^*,l+l_1N^*}\right| \\
&\quad\leq \sum_{\substack{k_1,l_1=-\infty\\(k_1,l_1)\neq(0,0)}}^{\infty}\frac{1}{16}h^4\pi^{-4}\sqrt{\frac{I_{k,l}}{L^2}}\frac{1}{\left((|k_1|-\frac{1}{2})^2+(|l_1|-\frac{1}{2})^2\right)^2}=C^*h^4\sqrt{\frac{I_{k,l}}{L^2}},
\end{aligned} \tag{B.6}$$

where

$$C^*=\frac{1}{16}\pi^{-4}\sum_{\substack{k_1,l_1=-\infty\\(k_1,l_1)\neq(0,0)}}^{\infty}\frac{1}{\left((|k_1|-\frac{1}{2})^2+(|l_1|-\frac{1}{2})^2\right)^2}. \tag{B.7}$$

Note that the double series

$$\sum_{\substack{k_1,l_1=-\infty\\(k_1,l_1)\neq(0,0)}}^{\infty}\frac{1}{\left((|k_1|-\frac{1}{2})^2+(|l_1|-\frac{1}{2})^2\right)^{\beta_0}}, \tag{B.8}$$

with $\beta_0=2$, is convergent. In turn, we arrive at

$$\begin{aligned}
&\sum_{k,l=-N}^{N}\left|\sum_{\substack{k_1,l_1=-\infty\\(k_1,l_1)\neq(0,0)}}^{\infty}\left(\lambda_{kx,(4)}+\frac{4(k+k_1N^*)^2\pi^2}{L^2}\right)\hat{f}_{k+k_1N^*,l+l_1N^*}\right|^2 \\
&\quad\leq \sum_{k,l=-N}^{N}(C^*)^2h^8\cdot\frac{I_{k,l}}{L^2}=\frac{(C^*)^2}{L^2}h^8\sum_{k,l=-N}^{N}I_{k,l}=\frac{(C^*)^2}{L^2}h^8\left\|\Delta^3 f\right\|^2 \\
&\quad= \frac{(C^*)^2}{L^2}h^8\left\|f\right\|_{H^6}^2,
\end{aligned} \tag{B.9}$$

in which the decomposition (B.1) was used in the second to the last step. Therefore, the first inequality of Lemma 2.7 is proven by taking $C_2 = \frac{(C^*)^2}{L^2}$. The second inequality of Lemma 2.7 can be established in the same manner. This completes the proof of Lemma 2.7.

# C Proof of Lemma 3.2

*Proof.* For any periodic grid function $f$, it has a corresponding discrete Fourier transformation:

$$f_{i,j} = \sum_{\ell,m=-N}^{N} \hat{f}^N_{\ell,m} \mathrm{e}^{2\pi i(\ell x_i + m y_j)/L}, \tag{C.1}$$

where $x_i = (i - \frac{1}{2})h$, $y_j = (j - \frac{1}{2})h$, and $\hat{f}^N_{\ell,m}$ are the coefficients. In turn, for an application of the operator $-\Delta_{h,(4)}$ to $f$, the following discrete Fourier expansion is available:

$$-\Delta_h f_{i,j} = \sum_{\ell,m=-N}^{N} (\nu_\ell + \nu_m) \hat{f}^N_{\ell,m} \mathrm{e}^{2\pi i(\ell x_i + m y_j)/L}, \tag{C.2}$$

$$-\Delta_{h,(4)} f_{i,j} = \sum_{\ell,m=-N}^{N} \Lambda_{\ell,m} \hat{f}^N_{\ell,m} \mathrm{e}^{2\pi i(\ell x_i + m y_j)/L}, \tag{C.3}$$

$$\text{with } \nu_k = \frac{4\sin^2 \frac{\ell\pi h}{L}}{h^2},\ \mu_k = \nu_k^2 + \frac{h^2}{12}\nu_k^2,\ \Lambda_{\ell,m} = \mu_\ell + \mu_m. \tag{C.4}$$

For any $f \in \mathring{\mathcal{V}}_{\mathrm{per}}$, we observe that $\hat{f}^N_{\ell,m} = 0$, due to the fact that $\overline{f} = 0$. In turn, a similar expansion could be derived for $(-\Delta_{h,(4)})^{-1} f$:

$$(-\Delta_{h,(4)})^{-1} f_{i,j} = \sum_{\ell,m\neq(0,0)} \Lambda^{-1}_{\ell,m} \hat{f}^N_{\ell,m} \mathrm{e}^{2\pi i(\ell x_i + m y_j)/L}. \tag{C.5}$$

On the other hand, the following identities could be derived, based on the orthonormal property of the Fourier basis function:

$$\|\|f\|^2_{-1,h} = (f, (-\Delta_{h,(4)})^{-1} f)_2 = L^2 \sum_{\ell,m\neq(0,0)} \Lambda^{-1}_{\ell,m} |\hat{f}^N_{\ell,m}|^2, \tag{C.6}$$

$$\|\nabla_{h,(4)} f\|_2^2 = (f, -\Delta_{h,(4)} f)_2 = L^2 \sum_{\ell,m\neq(0,0)} \Lambda_{\ell,m} |\hat{f}^N_{\ell,m}|^2, \tag{C.7}$$

for any $f \in \mathring{\mathcal{V}}_{\mathrm{per}}$. Meanwhile, an application of Parseval equality to (C.1) implies that

$$\|\|f\|^2 = L^2 \sum_{\ell,m\neq(0,0)} |\hat{f}^N_{\ell,m}|^2. \tag{C.8}$$

An application of discrete Cauchy-Schwarz inequality leads to

$$\left( \sum_{\ell,m\neq(0,0)} |\hat{f}^N_{\ell,m}|^2 \right)^2 \leq \left( \sum_{\ell,m\neq(0,0)} \Lambda^{-1}_{\ell,m} |\hat{f}^N_{\ell,m}|^2 \right) \cdot \left( \sum_{\ell,m\neq(0,0)} \Lambda_{\ell,m} |\hat{f}^N_{\ell,m}|^2 \right), \tag{C.9}$$

which is equivalent to $\|f\|_2^4 \leq \|f\|^2_{-1,h} \cdot \|\nabla_{h,(4)} f\|_2^2$, for any $f \in \mathring{\mathcal{V}}_{\mathrm{per}}$. This completes the proof of (3.7).

The proof of (3.8) follows a similar argument. By making a comparison between (C.2) and (C.3), combined with an application of Parseval equality, we get

$$\|\Delta_h f\|_2^2 = L^2 \sum_{\ell,m=-N}^{N} (\nu_\ell + \nu_m)^2 |\hat{f}_{\ell,m}^N|^2, \tag{C.10}$$

$$\|\Delta_{h,(4)} f\|_2 = L^2 \sum_{\ell,m=-N}^{N} \Lambda_{\ell,m}^2 |\hat{f}_{\ell,m}^N|^2. \tag{C.11}$$

Therefore, (3.8) becomes a direct consequence of the following fact:

$$|\nu_\ell + \nu_m| = \nu_\ell + \nu_m \le \Lambda_{\ell,m} = |\Lambda_{\ell,m}|. \tag{C.12}$$

The proof of Lemma 3.2 is finished. □

## Acknowledgements

This work is supported in part by the grants NSF DMS-1418689 (C. Wang), NSF DMS-1418692 and NSF DMS-1719854 (S. Wise).

## References

[1] J. Barrett and J. Blowey. Finite element approximation of the Cahn-Hilliard equation with concentration dependent mobility. *Math. Comp.*, 68:487–517, 1999.

[2] J. Barrett, J. Blowey, and H. Garcke. Finite element approximation of the Cahn-Hilliard equation with degenerate mobility. *SIAM J. Numer. Anal.*, 37:286–318, 1999.

[3] A. Baskaran, Z. Hu, J. Lowengrub, C. Wang, S.M. Wise, and P. Zhou. Energy stable and efficient finite-difference nonlinear multigrid schemes for the modified phase field crystal equation. *J. Comput. Phys.*, 250:270–292, 2013.

[4] A. Baskaran, J. Lowengrub, C. Wang, and S. Wise. Convergence analysis of a second order convex splitting scheme for the modified phase field crystal equation. *SIAM J. Numer. Anal.*, 51:2851–2873, 2013.

[5] J.P. Boyd. *Chebyshev and Fourier spectral methods*. Courier Corporation, 2001.

[6] J.W. Cahn and J.E. Hilliard. Free energy of a nonuniform system. i. interfacial free energy. *J. Chem. Phys.*, 28:258–267, 1958.

[7] C. Canuto and A. Quarteroni. Approximation results for orthogonal polynomials in Sobolev spaces. *Math. Comp.*, 38:67–86, 1982.

[8] W. Chen, S. Conde, C. Wang, X. Wang, and S.M. Wise. A linear energy stable scheme for a thin film model without slope selection. *J. Sci. Comput.*, 52:546–562, 2012.

[9] W. Chen, W. Feng, Y. Liu, C. Wang, and S.M. Wise. A second order energy stable scheme for the Cahn-Hilliard-Hele-Shaw equation. *Discrete Contin. Dyn. Sys. B*, 2018. Accepted and published online.

[10] W. Chen, Y. Liu, C. Wang, and S.M. Wise. An optimal-rate convergence analysis of a fully discrete finite difference scheme for Cahn-Hilliard-Hele-Shaw equation. *Math. Comp.*, 85:2231–2257, 2016.

[11] W. Chen, C. Wang, X. Wang, and S.M. Wise. A linear iteration algorithm for energy stable second order scheme for a thin film model without slope selection. *J. Sci. Comput.*, 59:574–601, 2014.

[12] K. Cheng, W. Feng, S. Gottlieb, and C. Wang. A Fourier pseudospectral method for the "Good" Boussinesq equation with second-order temporal accuracy. *Numer. Methods Partial Differential Equations*, 31(1):202–224, 2015.

[13] K. Cheng, C. Wang, S.M. Wise, and X. Yue. A second-order, weakly energy-stable pseudospectral scheme for the Cahn-Hilliard equation and its solution by the homogeneous linear iteration method. *J. Sci. Comput.*, 69:1083–1114, 2016.

[14] A. Diegel, X. Feng, and S.M. Wise. Convergence analysis of an unconditionally stable method for a Cahn-Hilliard-Stokes system of equations. *SIAM J. Numer. Anal.*, 53:127–152, 2015.

[15] A. Diegel, C. Wang, X. Wang, and S.M. Wise. Convergence analysis and error estimates for a second order accurate finite element method for the Cahn-Hilliard-Navier-Stokes system. *Numer. Math.*, 137:495–534, 2017.

[16] A. Diegel, C. Wang, and S.M. Wise. Stability and convergence of a second order mixed finite element method for the Cahn-Hilliard equation. *IMA J. Numer. Anal.*, 36:1867–1897, 2016.

[17] Q. Du and R. Nicolaides. Numerical analysis of a continuum model of a phase transition. *SIAM J. Numer. Anal.*, 28:1310–1322, 1991.

[18] C.M. Elliott and D.A. French. Numerical studies of the Cahn-Hilliard equation for phase separation. *IMA J. Numer. Anal.*, 38:97–128, 1987.

[19] C.M. Elliott and D.A. French. A nonconforming finite-element method for the two-dimensional Cahn-Hilliard equation. *SIAM J. Numer. Anal.*, 26:884–903, 1989.

[20] C.M. Elliott, D.A French, and F.A. Milner. A second-order splitting method for the Cahn-Hilliard equation. *Numer. Math.*, 54:575–590, 1989.

[21] C.M. Elliott and T. Ranner. Evolving surface finite element method for the Cahn-Hilliard equation. *Numer. Math.*, 129:483534, 2015.

[22] C.M. Elliott and A.M. Stuart. The global dynamics of discrete semilinear parabolic equations. *SIAM J. Numer. Anal.*, 30:1622–1663, 1993.

[23] C.M. Elliott and S. Zheng. On the Cahn-Hilliard equation. *Arch. Rational Mech. Anal.*, 96:339–357, 1986.

[24] D. Eyre. Unconditionally gradient stable time marching the Cahn-Hilliard equation. In J. W. Bullard, R. Kalia, M. Stoneham, and L.Q. Chen, editors, *Computational and Mathematical Models of Microstructural Evolution*, volume 53, pages 1686–1712, Warrendale, PA, USA, 1998. Materials Research Society.

[25] A. Fathy, C. Wang, J. Wilson, and S. Yang. A fourth order difference scheme for the maxwell equations on yee grid. *J. Hyperbol. Differ. Eq.*, 5(03):613–642, 2008.

[26] W. Feng, A.J. Salgado, C. Wang, and S.M. Wise. Preconditioned steepest descent methods for some nonlinear elliptic equations involving p-Laplacian terms. *J. Comput. Phys.*, 334:45–67, 2017.

[27] W. Feng, C. Wang, S.M. Wise, and Z. Zhang. A second-order energy stable Backward Differentiation Formula method for the epitaxial thin film equation with slope selection. *Numer. Methods Partial Differ. Equ.*, 2018. Accepted and in press.

[28] X. Feng and A. Prohl. Error analysis of a mixed finite element method for the Cahn-Hilliard equation. *Numer. Math.*, 99:47–84, 2004.

[29] X. Feng and S.M. Wise. Analysis of a fully discrete finite element approximation of a Darcy-Cahn-Hilliard diffuse interface model for the Hele-Shaw flow. *SIAM J. Numer. Anal.*, 50:1320–1343, 2012.

[30] B. Fornberg. Generation of finite difference formulas on arbitrarily spaced grids. *Math. Comp.*, 51(184):699–706, 1988.

[31] B. Fornberg. Classroom note: Calculation of weights in finite difference formulas. *SIAM review*, 40(3):685–691, 1998.

[32] D. Furihata. A stable and conservative finite difference scheme for the Cahn-Hilliard equation. *Numer. Math.*, 87:675–699, 2001.

[33] D. Gottlieb and S. A. Orszag. *Numerical analysis of spectral methods: theory and applications*. SIAM, 1983.

[34] Z. Guan, J.S. Lowengrub, and C. Wang. Convergence analysis for second order accurate schemes for the periodic nonlocal Allen-Cahn and Cahn-Hilliard equations. *Math. Methods Appl. Sci.*, 40(18):6836–6863, 2017.

[35] Z. Guan, J.S. Lowengrub, C. Wang, and S.M. Wise. Second-order convex splitting schemes for nonlocal Cahn-Hilliard and Allen-Cahn equations. *J. Comput. Phys.*, 277:48–71, 2014.

[36] Z. Guan, C. Wang, and S.M. Wise. A convergent convex splitting scheme for the periodic nonlocal Cahn-Hilliard equation. *Numer. Math.*, 128:377–406, 2014.

[37] J. Guo, C. Wang, S.M. Wise, and X. Yue. An $H^2$ convergence of a second-order convex-splitting, finite difference scheme for the three-dimensional Cahn-Hilliard equation. *Commu. Math. Sci.*, 14:489–515, 2016.

[38] D. Han and X. Wang. A second order in time, uniquely solvable, unconditionally stable numerical scheme for Cahn-Hilliard-Navier-Stokes equation. *J. Comput. Phys.*, 290:139–156, 2015.

[39] Y. He, Y. Liu, and T. Tang. On large time-stepping methods for the Cahn-Hilliard equation. *Appl. Numer. Math.*, 57(4):616–628, 2006.

[40] J. S. Hesthaven, S. Gottlieb, and D. Gottlieb. *Spectral methods for time-dependent problems*, volume 21. Cambridge University Press, 2007.

[41] Z. Hu, S. Wise, C. Wang, and J. Lowengrub. Stable and efficient finite-difference nonlinear-multigrid schemes for the phase-field crystal equation. *J. Comput. Phys.*, 228:5323–5339, 2009.

[42] A. Iserles. *A first course in the numerical analysis of differential equations*, volume 44. Cambridge University Press, 2009.

[43] D. Kay and R. Welford. A multigrid finite element solver for the Cahn-Hilliard equation. *J. Comput. Phys.*, 212:288–304, 2006.

[44] D. Kay and R. Welford. Efficient numerical solution of Cahn-Hilliard-Navier-Stokes fluids in 2D. *SIAM J. Sci. Comput.*, 29:2241–2257, 2007.

[45] N. Khiari, T. Achouri, M.L. Ben Mohamed, and K. Omrani. Finite difference approximate solutions for the Cahn-Hilliard equation. *Numer. Meth. PDE*, 23:437–455, 2007.

[46] J.S. Kim, K. Kang, and J.S. Lowengrub. Conservative multigrid methods for Cahn-Hilliard fluids. *J. Comput. Phys.*, 193:511–543, 2003.

[47] C. Lee, D. Jeong, J. Shin, Y. Li, and J. Kim. A fourth-order spatial accurate and practically stable compact scheme for the Cahn-Hilliard equation. *Physica A*, 409:17–28, 2014.

[48] D. Li and Z. Qiao. On second order semi-implicit Fourier spectral methods for 2D Cahn-Hilliard equations. *J. Sci. Comput.*, 70:301–341, 2017.

[49] J. Li, Z. Sun, and X. Zhao. A three level linearized compact difference scheme for the Cahn-Hilliard equation. *Sci. China Math.*, 55:805–826, 2012.

[50] Y. Li, H. Lee, B. Xia, and J. Kim. A compact fourth-order finite difference scheme for the three-dimensional Cahn-Hilliard equation. *Comput. Phys. Commun.*, 200:108–116, 2016.

[51] C. Liu and J. Shen. A phase field model for the mixture of two incompressible fluids and its approximation by a Fourier-spectral method. *Physica D*, 179:211–228, 2003.

[52] J.-G. Liu and C. Wang. A fourth order numerical method for the primitive equations formulated in mean vorticity. *Commun. Comput. Phys*, 4:26–55, 2008.

[53] J.-G. Liu, C. Wang, and H. Johnston. A fourth order scheme for incompressible Boussinesq equations. *J. Sci. Comput.*, 18(2):253–285, 2003.

[54] Y. Liu, W. Chen, C. Wang, and S.M. Wise. Error analysis of a mixed finite element method for a Cahn-Hilliard-Hele-Shaw system. *Numer. Math.*, 135:679–709, 2017.

[55] S.A. Orszag and C.M. Bender. Advanced mathematical methods for scientists and engineers. *Mac Graw Hill*, 1978.

[56] R. Samelson, R. Temam, C. Wang, and S. Wang. A fourth-order numerical method for the planetary geostrophic equations with inviscid geostrophic balance. *Numer. Math.*, 107(4):669–705, 2007.

[57] J. Shen, C. Wang, X. Wang, and S.M. Wise. Second-order convex splitting schemes for gradient flows with Ehrlich-Schwoebel type energy: Application to thin film epitaxy. *SIAM J. Numer. Anal.*, 50:105–125, 2012.

[58] H. Song. Energy stable and large time-stepping methods for the Cahn-Hilliard equation. *Inter. J. Comput. Math.*, 92:2091–2108, 2015.

[59] E. Tadmor. The exponential accuracy of fourier and chebyshev differencing methods. *SIAM J. Numer. Anal.*, 23:1–10, 1986.

[60] C. Wang, J.-G. Liu, and H. Johnston. Analysis of a fourth order finite difference method for the incompressible Boussinesq equations. *Numer. Math.*, 97(3):555–594, 2004.

[61] C. Wang, X. Wang, and S.M. Wise. Unconditionally stable schemes for equations of thin film epitaxy. *Discrete Contin. Dyn. Sys. A*, 28:405–423, 2010.

[62] C. Wang and S.M. Wise. An energy stable and convergent finite-difference scheme for the modified phase field crystal equation. *SIAM J. Numer. Anal.*, 49:945–969, 2011.

[63] T. Wang, L. Zhao, and B. Guo. A class of stable and conservative finite difference schemes for the Cahn-Hilliard equation. *Acta Math. Appl. Sin. Engl. Ser.*, 31:863–878, 2015.

[64] S.M. Wise. Unconditionally stable finite difference, nonlinear multigrid simulation of the Cahn-Hilliard-Hele-Shaw system of equations. *J. Sci. Comput.*, 44:38–68, 2010.

[65] S.M. Wise, J.S. Kim, and J.S. Lowengrub. Solving the regularized, strongly anisotropic Chan-Hilliard equation by an adaptive nonlinear multigrid method. *J. Comput. Phys.*, 226:414–446, 2007.

[66] S.M. Wise, C. Wang, and J.S. Lowengrub. An energy stable and convergent finite-difference scheme for the phase field crystal equation. *SIAM J. Numer. Anal.*, 47:2269–2288, 2009.

[67] Y. Yan, W. Chen, C. Wang, and S.M. Wise. A second-order energy stable BDF numerical scheme for the Cahn-Hilliard equation. *Commun. Comput. Phys.*, 23:572–602, 2018.